


A Search of Potential Drugs for Alzheimer's Disease: Investigation of Cholinergic Inhibition by Gepant Derivatives through Computational Techniques

Karthikeyan Asokan¹ , Mahendiraprabu Ganesan¹ , Abiram Angamuthu² ,
Selvarengan Paranthaman^{1,*} 

¹ Department of Physics and International Research Centre, Kalasalingam Academy of Research and Education (Deemed to be University), Krishnankoil 626 126, India; a.karthikeyan@klu.ac.in (K.A.); mahendiraprabhu@klu.ac.in (M.G.);

² Department of Physics, PSG College of Arts and Science, Coimbatore 641014, India; aabiram@psgcas.ac.in (A.A.);

* Correspondence: psrengan@hotmail.com (S.P.);

Received: 25.03.2024; Accepted: 1.01.2025; Published: 20.12.2025

Abstract: Alzheimer's disease is widely recognized as a common type of disease among older adults. Although the cause of the disease is unknown, a few hypotheses have been reported in the literature. Among them, cholinergic inhibition has received recent attention. In the present investigation, cholinergic inhibition by gepant derivatives is examined through computational techniques. The molecular geometries of the selected gepant derivatives are optimized using the density functional theory (B3LYP/6-31G*) method. These studies are performed to foresee the binding interactions of gepant derivatives with acetylcholinesterase (AChE) and butyrylcholinesterase (BuChE). The gepant derivatives such as Atogepant, Rimegepant, Ubrogapant, and MK-3207 are selected for the study. The structural stability, reactivity, and other molecular parameters are calculated for the selected ligands. The calculated energy gap values of Rimegepant and MK-3207 are 5.10 eV and 4.97 eV, respectively. Furthermore, a molecular electrostatic potential (MEP) study was employed to identify electron-rich and electron-poor reactive sites and to characterize the bonding properties of the gepant derivatives. The binding mechanisms of the selected ligands to AChE and BuChE are investigated using molecular docking and molecular dynamics methods. Finally, the gepant derivatives' reactive parameters, stability, and binding energies are compared with those of standard cholinesterase compounds. Our computational studies revealed that rimegepant and MK-3207 are active compounds with strong binding energies against AChE (-11.7 kcal/mol) and BuChE (-12.0 kcal/mol), respectively. Our studies indicate that these compounds are good inhibitors of AChE and BuChE. Hence, it is concluded that Rimegepant and MK-3207 are potential drug candidates for the design of a new drug against AD.

Keywords: Alzheimer's disease; acetylcholinesterase; gepant derivatives; density functional theory; molecular docking.

© 2025 by the authors. This article is an open-access article distributed under the terms and conditions of the Creative Commons Attribution (CC BY) license (<https://creativecommons.org/licenses/by/4.0/>), which permits unrestricted use, distribution, and reproduction in any medium, provided the original work is properly cited. The authors retain copyright of their work, and no permission is required from the authors or the publisher to reuse or distribute this article, as long as proper attribution is given to the original source.

1. Introduction

Alzheimer's disease (AD), a neurodegenerative disorder, causes neuronal loss, impairment of memory, and loss of synapses [1–3]. It is one of the most prevalent types of dementia that affects elderly persons. The World Health Organization (WHO) recently published a fact sheet stating that AD affects more than 55 million individuals globally [4–6].

Though the disease's cause is unknown, a few hypotheses and a few mechanisms were outlined in the literature. They are glycogen synthase kinase 3 (GSK3) hypothesis [7,8], calcium hypothesis [9,10], oxidative stress hypothesis [11,12], mitochondrial cascades and related hypotheses [13,14], apolipoprotein E [15], β -secretase (BACE1) [16,17], monoamine oxidase (MAO) [18,19], cholinergic hypothesis, and metal ions level in different brain regions [20]. Herein, the cholinergic hypothesis has received recent attention from scientists. Earlier studies have shown that acetylcholinesterase (AChE) inhibitors may raise acetylcholine (ACh) levels in AD patients by inhibiting AChE [21,22].

The drugs that are currently available for the use of pharmacotherapy of AD are galantamine, memantine, rivastigmine, and donepezil [23,24]. All these medications are AChE inhibitors except memantine. Donepezil hydrochloride, as the second approved drug by the United States Food and Drug Administration (FDA) for the treatment of moderate AD, is a dual-binding inhibitor of AChE [25–27]. The currently available drugs for AD cause side effects such as vomiting, nausea, loss of appetite, diarrhea, sleep problems, muscle pain, headaches, feeling tired, itching or a rash, dizziness, hallucinations, aggression, etc [28]. In order to avoid the side effects, it is necessary to find alternate and appropriate drugs to cure AD. Recently, drug repurposing has attracted the attention of scientists, leading to an enormous number of studies reported in the literature [29,30]. In general, drug repurposing often seeks to find additional targets for already prescribed medications. For instance, Itraconazole, a medicine originally intended to treat fungal infections, also shows anticancer properties against prostate and lung cancer [31,32]. Drug repurposing is regarded as a significant area of drug discovery because it helps to avoid problems with optimization that arise during drug discovery, development, and preclinical testing. Further, the pharmacological and toxicological data for already-approved medications enable quicker, less expensive repositioning [33,34].

Biomarker derivatives, such as Amyloid-beta ($A\beta$) plaques, are protein aggregates found in the brains of Alzheimer's patients and are key to AD diagnostics. $A\beta_{40}$ accounts for over 80% of $A\beta$ in the normal human brain, while excess $A\beta_{42}$ accumulates as amyloid plaques in pathological conditions. $A\beta_{42}$ shows higher neurotoxicity and faster aggregation kinetics than $A\beta_{40}$. The natural unfolded state of $A\beta$ undergoes a slow transition into a partially folded state (β -sheet) [35]. Hyperphosphorylated tau protein derivatives lead to neurofibrillary tangles, another hallmark of AD [36]. Neurofilament light chain (NfL) is a marker of neurodegeneration used to monitor the rate of neuronal damage in AD. These two lesions are caused by the dysfunction and the accumulation of two proteins [37]. Anti-amyloid drugs aim to reduce $A\beta$ buildup, which helps clear amyloid plaques. Anti-tau therapies aim to inhibit or modify the tau protein pathology. Other derivatives include genetic, stem cell, neuroimaging, and model derivatives. Among them, Cholinesterase inhibitors received special attention (e.g., donepezil, rivastigmine, and galantamine) because they are among the earliest cholinesterase inhibitor molecules [38].

Recently, Morton *et al.* revealed that migraines were a significant risk factor for AD [39]. The drugs that can be used to treat migraines are gepant derivatives such as Atogepant, Rimegepant, Ubrogepant, and MK-3207 [40–42]. To the best of our knowledge, no systematic study of cholinergic inhibition by gepant derivatives has been conducted. Hence, in the present study, we investigate the ability of migraine drugs to inhibit AChE and BuChE using computational techniques. In particular, using computational techniques, migraine medications are repurposed in this *in vitro* study to assess their potential anti-Alzheimer activity. We employ computational techniques, including quantum chemistry, molecular docking, and molecular

dynamics, to investigate cholinergic inhibition by gepant derivatives. In particular, the biological activity of these derivatives towards AChE and BuChE is evaluated. Among these two, AChE is responsible for the hydrolysis of ACh, and BuChE's role is not clearly known. In patients with neurodegenerative abnormalities, it is thought to have a compensatory role in the progression of ACh hydrolysis in the brain. The selected gepant derivatives are Atogepant, Rimegepant, Ubrogapant, and MK-3207. These derivatives are used in the study, inspired by the structures of rivastigmine and donepezil. Further, our computational studies are extended to currently available drug molecules for AD for comparison purposes. Quantum-chemical calculations are performed to study the structures and molecular properties of the above ligands. The optimized ligands are docked with AChE and BuChE, and their docking properties are studied. The docking study is performed to understand the allosteric binding modes of the above-mentioned ligands with the enzyme. The allosteric nature of AChE and BuChE inhibition by these compounds provides an opportunity to design subtype-selective enzyme inhibitors. Molecular dynamics simulations are performed to understand the binding mechanism and stability of the selected gepant derivatives towards AChE and BuChE under experimental conditions or in a real-time environment. Finally, we hope our combined study of quantum chemistry, docking, and dynamics will be helpful in designing novel anti-Alzheimer agents.

2. Materials and Methods

The experimental geometries of gepant derivatives such as Atogepant (Pubchem ID: 72163100), Rimegepant (Pubchem ID: 51049968), Ubrogapant (Pubchem ID: 68748835), and MK-3207 (Pubchem ID: 25019940) are taken from Pubchem. Similarly, the molecular geometries of AD drugs such as Rivastigmine (Pubchem ID: 77991), Galantamine (Pubchem ID: 9651), and Donepezil (Pubchem ID: 3152) are also taken from PubChem. These molecular geometries are optimized using the density functional theory (DFT) method. In particular, all molecular geometries are optimized using the B3LYP functional with the 6-31G* basis set [43,44]. Reactivity properties, such as ionization energy, electron affinity, energy gap, chemical hardness, and chemical potential, are calculated from the highest occupied molecular orbital (HOMO) and lowest unoccupied molecular orbital (LUMO) energies. A molecular electrostatic potential (MEP) map is also generated. HOMO, LUMOs, and MEP maps are generated using the GaussView 5 program [45]. All the DFT calculations are performed using the Gaussian09W program [46].

The docking study is performed for all the selected gepant and AD drug molecules against AChE and BuChE. Recently reported crystal structures of AChE (PDB ID. 7E3D) and BuChE (PDB ID. 1P0I) are taken from the protein data bank (Figure 1a). In addition, AChE and BChE have been proposed as a link to the well-recognized association with Alzheimer's disease. Both proteins are derived from the human organism (*homo sapiens*). We chose 7E3D and 1P0I because they have the highest-resolution structures of Human AChE and BuChE without substrate. Standard cleaning procedures were followed before the docking. That is, ligands and water molecules are removed, and polar hydrogens are in AChE and BuChE. The docking complexes are studied based on their binding energy values. All molecular docking study is performed using the PyRx 0.8 program [47]. The best poses of the interaction between ligand-protein complexes are visualized using Discovery Studio Visualizer v19.1.0.18287 [48].

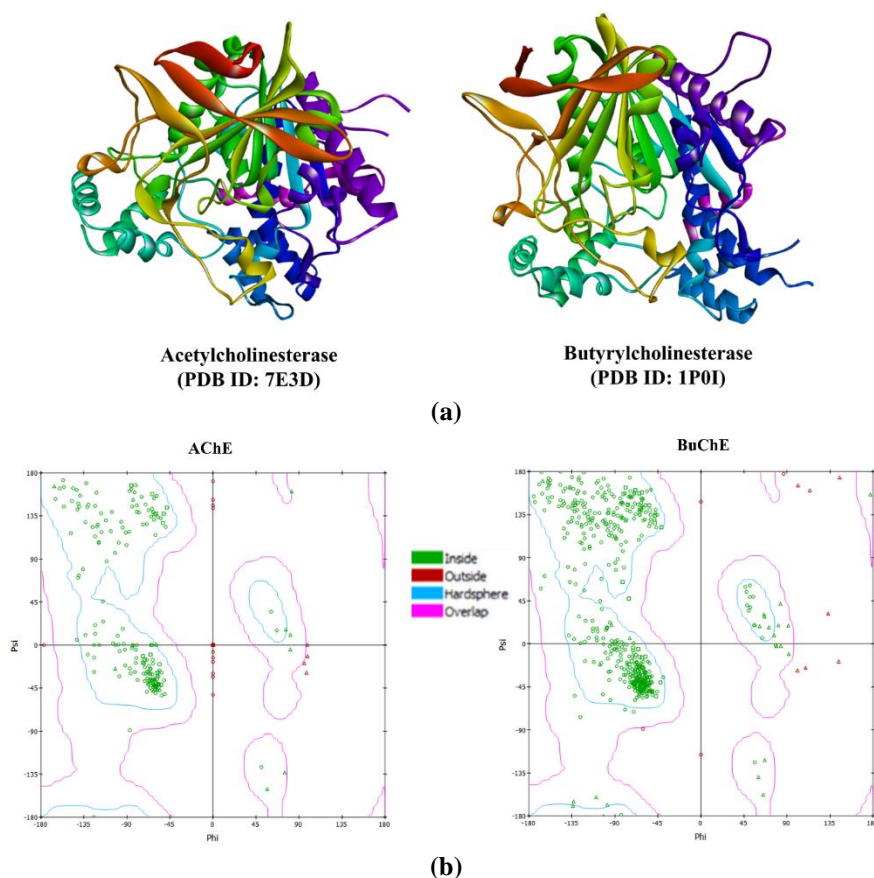


Figure 1. (a) Crystal structure of acetylcholinesterase and butyrylcholinesterase; (b) Ramachandran plot for AChE (7E3D) and BuChE (1P0I).

Every residue also has two freely rotating bonds. These two angles, ψ (psi) and ϕ (phi), are known as the Ramachandran angles, and they specify the shape of that residue in a protein. Analysing Ramachandran plots of the backbone angles for the AChE and BuChE structural models revealed that both lie within the regions of psi–phi space frequently observed in Figure 1b. From Figure 1b, it can be seen that most amino acid residues are within allowed regions, confirming that the AChE and BuChE protein structures are of good conformational quality. To understand the inhibition mechanism in a real-time or experimental environment, Molecular Dynamics (MD) simulations are performed. In general, MD studies are performed to understand the conformational stability of proteins or biomolecules. In particular, the stability of protein-ligand complexes is investigated using MD. The trajectory files are generated for the given protein-ligand system using MD. The dynamic study of all selected protein-ligand complexes is performed using the COSMO-Surface gene in the mypresto portal ver. 1.1.86 with AMBER ff99SB force field [49]. As a preliminary step, the selected protein-ligand complex was immersed in a cubic box, and the TIP3P water model was used to solvate the system. A temperature of 300 K was maintained for all simulations. The MD simulation is performed for 2 ns due to computational limitations. Initial geometries of selected ligands and proteins for the MD study are taken from PubChem and PDB, respectively.

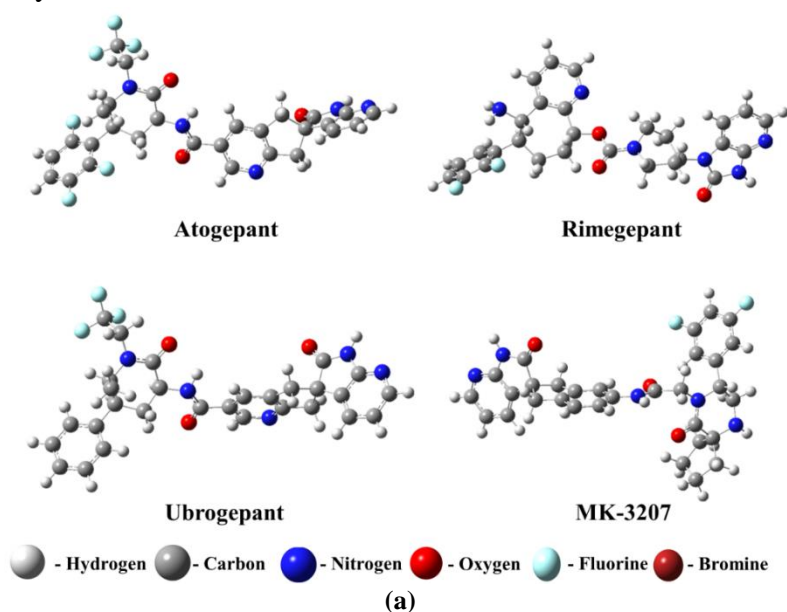
3. Results and Discussion

3.1. Structure.

Quantum chemical calculations are performed to obtain more detailed molecular-level information on the selected gellant derivatives. All the gellant derivatives, along with the AD

drug molecules, are optimized using the B3LYP functional with the 6-31G* basis set (Figures 2a and 2b). Computational tools such as DFT, molecular docking, and molecular dynamics are efficient and cost-effective for understanding biological molecules and drugs. Atogepants, which block CGRP, a protein associated with migraine pathophysiology, can help prevent the inflammation and pain that trigger migraines. Structurally, Atogepant consists of pyridine, piperidine, benzyl, amino, and carboxylic groups. Three fluorine atoms are also bonded to a benzene ring. These functional groups/rings are favorable sites for the noncovalent interactions with the specific region in the enzyme. Noncovalent interactions, such as hydrogen bonding, van der Waals interactions, and π - π interactions, can occur when these ligands bind to the enzyme. Rimegepant is another medication used for the treatment of migraines, but it has a dual role: it can be used for both acute treatment and preventive treatment of migraines. Like atogepant, it belongs to the class of CGRP receptors. Similarly, Rimegepant consists of benzyl, piperidine, and indanone regions along with amino and carboxylic groups. Further, it also consists of two F atoms bonded to a benzene ring.

Unlike atogepant and rimegepant, ubrogepant is not used for the prevention of migraines but is specifically intended to stop ongoing migraine pains. Ubrogapants consist of benzyl, piperidine, and indanone regions, along with amino and carboxylic groups. It also consists of three F atoms bonded to a benzene ring. MK-3207 was shown to be effective at relieving migraine pain. Similar to other CGRP receptors, it had a rapid onset and sustained migraine relief. MK-3207 consists of benzyl, piperidine, and indanone regions along with amino and carboxylic groups. It consists of two F atoms bonded to a benzene ring. All the studied gepant derivatives consist of electronegative elements such as O, N, F, or Br, as well as benzene rings. This indicates that these ligands are favorable for intermolecular noncovalent interactions such as hydrogen bonds and π - π interactions. These derivatives readily form noncovalent bond interactions with AChE and BuChE. In addition, the presence of electronegative elements in the ligand will increase the lipophilicity, which increases the metabolic activity and membrane permeation of the ligand molecule [50]. Similarly, indanone, benzyl, piperidine, amino, and carboxylic functional groups are present in AD drug molecules. These groups are favorable for the formation of noncovalent interactions between AD drug molecules and enzymes.



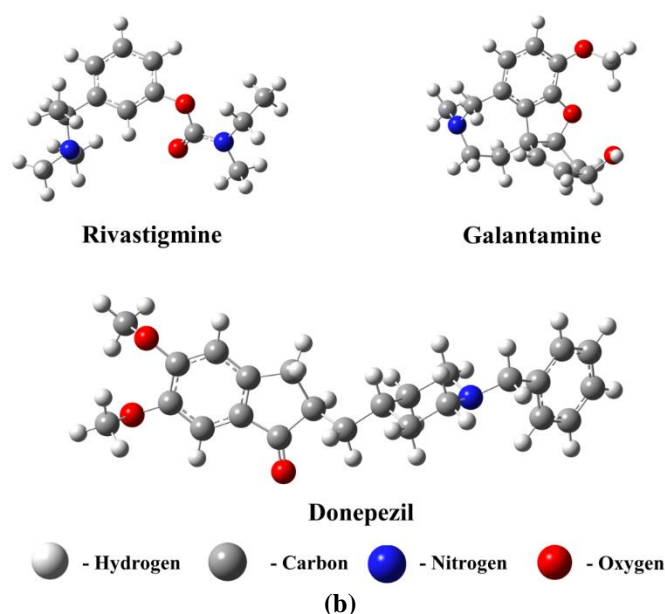


Figure 2. (a) The optimized structure of the selected gepant derivatives using B3LYP/6-31G* level of theory; (b) The optimized structure of the AD drugs using B3LYP/6-31G* level of theory.

The three primary functional groups in donepezil are the dimethoxyindanone moiety, the piperidine group, and the benzyl group. Rivastigmine is made up of a carboxy group of ethyl (methyl) and carbamic acid with the phenolic OH group. The chemical structures of galantamine consist of four rings: an aromatic ring, a heterocyclic ring, a cyclohexenol ring, and an azepine ring. Donepezil is a medication used to treat AD and other forms of dementia. It works by inhibiting the enzyme AChE, which breaks down ACh, a neurotransmitter important for memory and learning. Rivastigmine is a medication used to treat mild to moderate AD and dementia. Like donepezil, it is a cholinesterase inhibitor. Galantamine is a medication used for the treatment of mild to moderate AD. It is a cholinesterase inhibitor like donepezil and rivastigmine, and it also has additional action as an allosteric modulator of nicotinic ACh receptors.

3.2. Reactivity parameters.

The highest occupied molecular orbital (HOMO) shows the electron donor nature, and the lowest unoccupied molecular orbital (LUMO) shows the electron receptor nature of the molecule. The energy gap between HOMO and LUMO represents the chemical stability, hardness, and softness of the molecule [51,52]. The frontier molecular orbital (FMO) analysis indicates the bioactivity of the selected ligand molecules. The FMOs of the studied ligand molecule are shown in Figures 3a and b. In Figures 3a and b, red and green indicate the positive and negative phases, respectively. The reactivity parameters of the studied ligands are listed in Table 1. In the case of Atogepant, the electrons are fully localized on the pyridine ring and partially localized on the pyrrole ring. In LUMO, the electrons are fully localized in the pyridine ring and the amino and carboxylic group (peptide bond); all other functional groups are free from localization. This clearly shows that intramolecular charge transfer occurs within the Atogepant molecule. The obtained energy gap value confirms the bioactive nature of the Atogepant. In the case of Rimegepant, both HOMO and LUMO electrons are localized in the pyridine and imidazole rings. In the case of Ubrogepant, HOMO electrons are localized at one end of the pyridine ring, and LUMO electrons are localized in the central pyridine ring. Similarly, in the case of MK-3207, HOMO electrons are localized in the peptide bond and

carboxylic group, whereas LUMO electrons are localized in the pyridine and imidazole ring. This indicates that electron localization will occur in either the pyridine or the imidazole group in most of the cases considered in this study. This shows that these functional groups are reactive and more favorable for forming noncovalent interactions with AChE and BuChE. In the case of AD drug molecules, it is commonly observed that the HOMO of electrons is localized in the amino group and the nearby methyl group in rivastigmine. In the case of LUMO, electrons are localized at the benzene ring and nearby functional groups. Similarly, HOMO and LUMO electrons are uniformly distributed. However, the electrons are localized in benzene, furan rings, and amino groups. In the case of HOMO of Donepezil, the electrons are localized at the benzene and the amino group. LUMO of Donepezil, the electrons are localized at other benzene rings and oxygen groups. This indicates that these functional groups are highly reactive and can readily interact with AChE and BuChE.

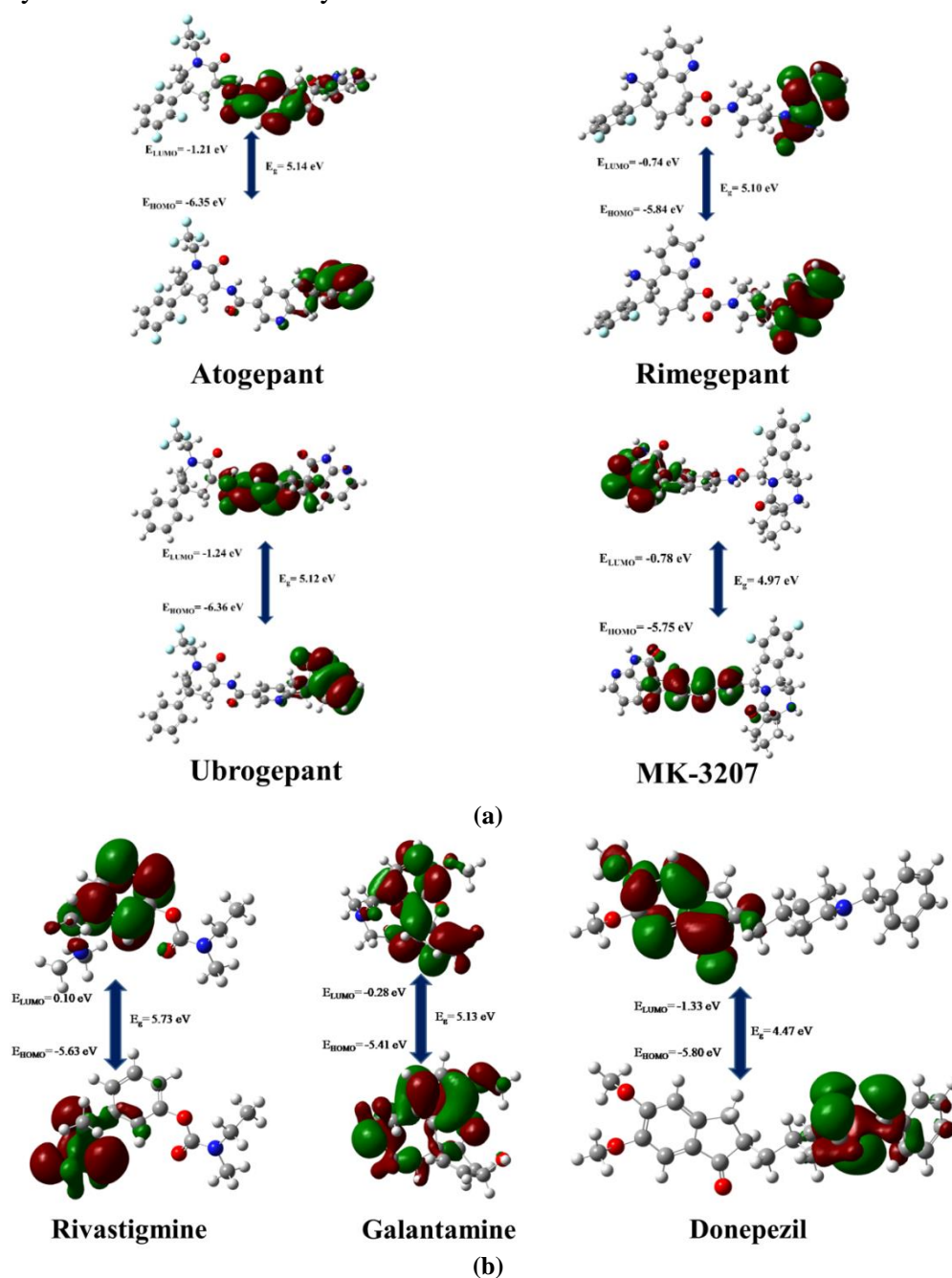


Figure 3. (a) HOMO to LUMO energy level diagrams of the gepant derivatives using B3LYP/6-31G* level of theory; (b) HOMO to LUMO energy level diagrams of the AD drugs using B3LYP/6-31G* level of theory.

The calculated reactivity parameters, including ionization energy, electron affinity, energy gap, chemical hardness, chemical potential, and dipole moment, are presented in Table 1. From Table 1, it can be seen that the calculated reactivity parameters of all the studied gepant derivatives are well aligned with those of the AD drug molecules considered in this study. A large energy gap corresponds to high stability and low chemical reactivity, whereas a tiny energy gap denotes low stability and high chemical reactivity. The calculated energy gap value is greater than 4 eV for all the studied gepant derivatives. This indicates that these compounds are highly stable. According to the maximum hardness principle, a molecule with a higher chemical hardness is more stable [53]. Chemicals with a smaller energy gap are considered softer due to their increased polarizability and molecular reactivity. Chemicals with a larger energy difference are typically more stable and have a higher molecular hardness. In our study, the same order of stability is observed in the energy gaps and chemical hardness values of gepant derivatives and AD drug molecules. That is, energy gap values show that the order of stability of gepant derivatives is Atogepant > Ubrogapant > Rimegepant > MK-3207. A similar trend is observed from chemical hardness values also. In AD drug molecules, the order of stability is Rivastigmine > Galantamine > Donepezil. This same order is also noted from chemical hardness values. In particular, the energy gap value varies from 4.47 eV (Donepezil) to 5.73 eV (Rivastigmine). The chemical hardness values range from 2.24 eV (Donepezil) to 2.87 eV (Rivastigmine) for all the studied compounds. All the gepant derivatives' energy gaps and chemical hardness values lie between those of Donepezil and Rivastigmine. The energy gap value varies from 4.97 eV (MK-3207) to 5.14 eV (Atogepant), and the chemical hardness value varies from 2.48 eV (MK-3207) to 2.52 eV (Ubrogapant). Among the studied gepant and AD drug molecules, MK-3207 and Donepezil are more reactive because they have smaller energy gaps and chemical hardness values. This is supported by the ionization energies and electron affinities of these compounds. It must be noted that the organic molecules have higher ionization energy. A similar trend is observed in the present study, also. The ionization energy value varies from 5.41 (Galantamine) to 6.36 eV (Ubrogapant). The calculated ionization energy is greater than 5 eV. Similarly, lower electron affinities were observed for the studied gepant derivatives and AD drug molecules. This indicates these molecules are highly stable.

Long-range electrostatic forces significantly impact the properties of biomolecules. These forces arise due to the presence of permanent electric dipole moments in the system. In the present study, we have calculated the dipole moment of the gepant derivatives and AD drug molecules to understand their solubility in the liquid phase. It must be noted that molecules with higher dipole moments are highly stable in the liquid state. From Table 1, it can be seen that the dipole moment value is large (9.20 Debye) for Ubrogapant and low (1.80 Debye) for rivastigmine. In summary, gepant derivatives considered in this study have a higher dipole moment. This indicates that these compounds are highly polar. The order of solubility is Ubrogapant > Atogepant > Rimegepant > Donepezil > Galantamine > MK-3207 > Rivastigmine.

Table 1. Calculated Ionization energy (I, eV), electron affinity (A, eV), energy gap (E_g , eV), chemical hardness (η , eV), chemical potential (μ , eV), and dipole moment (μ_B , eV).

Parameters	Atogepant	Rimegepant	Ubrogapant	MK-3207	Rivastigmine	Galantamine	Donepezil
I	6.35	5.84	6.36	5.75	5.63	5.41	5.80
A	1.21	0.74	1.24	0.78	-0.10	0.28	1.33
E_g	5.14	5.10	5.12	4.97	5.73	5.13	4.47
η	2.57	2.55	2.56	2.48	2.87	2.56	2.24
μ	3.78	3.29	3.80	3.26	2.76	2.84	3.56
μ_B	9.02	4.05	9.20	2.30	1.80	2.84	3.70

3.3. Molecular electrostatic potential.

The molecular electrostatic potential (MEP) analysis is used to estimate the chemical reactivity of molecules. Hydrogen-bonding (H-bond) sites, nucleophilic sites, and electrophilic sites were identified using this electron density-based analysis. The MEP map can be used to study the relationship between molecular structure and physicochemical properties [54–56]. That is, to understand the electrostatic effects arising from the charge distribution in the system, MEP can be used [57]. The MEP surfaces of the studied systems are shown in Figures 4a and 4b. The electrophiles and nucleophiles are shown in green and blue. The light blue color indicates the zero potential. From Figure 4, it can be seen that all oxygen atom sites correspond to the most negative potential region (dark red), whereas fluorine and nitrogen are colored blue or green. This indicates these sites are less negative regions. In general, these sites are more negative because they are electronegative. Large charge delocalization makes these sites less negative. Similarly, hydrogen atom sites are represented in light or dark blue, i.e., regions of positive potential. In the studied systems, green color predominates in most cases, indicating that these sites are electrophilic. Further, there are three electrophilic active centers in all gepant derivatives, two in rivastigmine, and three in Galantamine and Donepezil (Figure 4). These sites are more favorable for hydrogen-bonded interactions than the other sites.

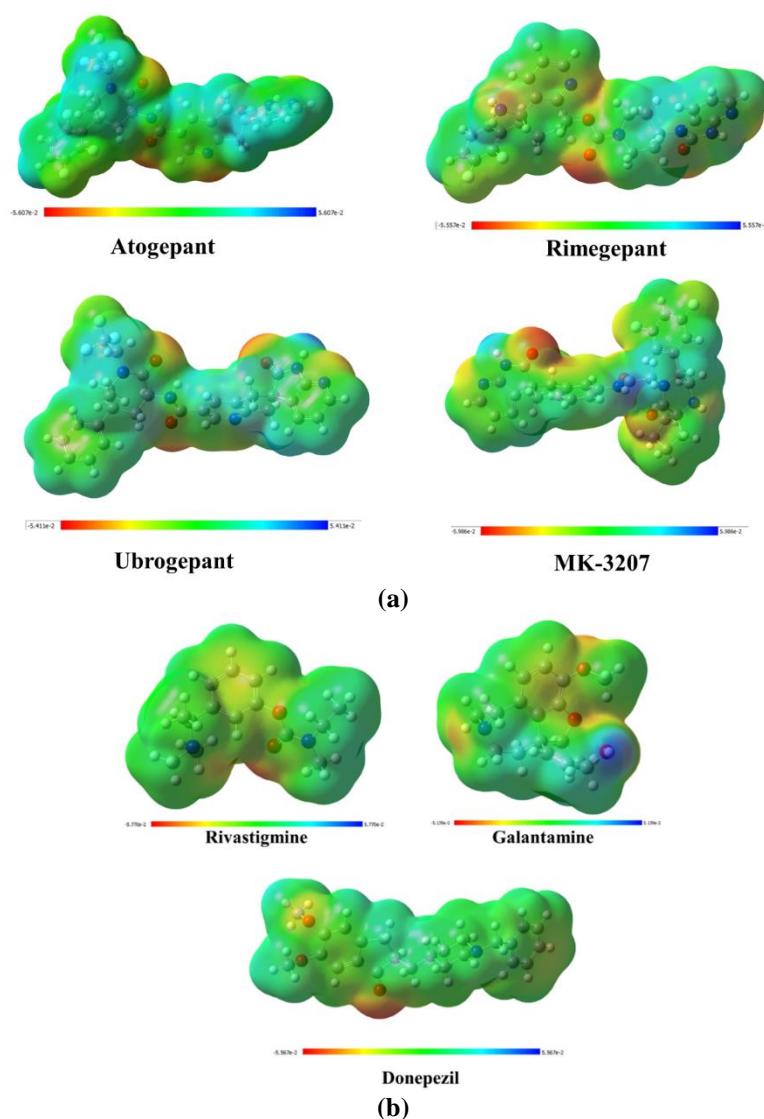


Figure 4. (a) Total density of MEP surface of the gepant derivatives using B3LYP/6-31G* level of theory.; (b) Total density of MEP surface of the AD drugs using B3LYP/6-31G* level of theory.

3.4. Molecular docking.

One of the most important computational tools for understanding protein-ligand interactions is *in silico* molecular docking. In general, molecular docking is used to study the ligand's allosteric binding mode and its biological effect on the enzyme. The molecular docking study is performed to determine the optimal binding modes in AChE and BuChE, as well as to identify the lead compound among the gepant derivatives considered in this study. Additionally, the important residues interacting with the targeted proteins' active sites were highlighted by this docked pose. The 2D images of various interactions of the three best possible allosteric binding modes (poses) of all the selected ligands with AChE (7E3D) and BuChE (1P0I) are given in Figures S1 and S2, respectively, in the supporting information file. Their binding energies are given in Table 2. The best docking poses and their 2D interactions for 7E3D with rimegepant and donepezil are shown in Figure 5. Similarly, the 2D interactions of 1P0I with MK-3207 and donepezil are shown in Figure 6. From Figure 5, it can be seen that both rimegepant and donepezil docks are at the same binding site in 7E3D. However, in the case of 1P0I, both MK-3207 and donepezil bind at different binding sites (Figure 6). Among the selected gepant derivatives, rimegepant has a higher binding energy (-11.7 kcal/mol) with 7E3D. However, in the case of 1P0I, gepant derivatives such as atogepant, rimegepant, and MK-3207 have similar binding energy values (Table 2). As mentioned earlier, rimegepant consists of benzyl, piperidine, and indanone regions along with carbamate groups. In addition, it also consists of two F atoms bonded to a benzene ring. There are three noncovalent interactions present in the 7E3D-rimegepant compound, and they are Pi-alkyl interaction (hydrophobic) with TYR18, hydrogen bond interaction (hydrophilic) with ASN19, and halogen (F) interaction (hydrophobic) with ASP20. Due to these interactions, rimegepant has a strong binding with 7E3D. That is, rimegepant has a strong interaction with the amino acid residues TYR18, ASN19, and ASP20 of 7E3D. Further, the functional groups present in MK-3207 are similar to rimegepant except for the carbamate group, which is present in rimegepant and absent in MK-3207. It also consists of two F atoms bonded to a benzene ring. There are four noncovalent interactions present in the 1P0I-MK-3207 compound. They are conventional hydrogen bonds, halogen, alkyl, Pi-Pi stacked, and Pi-alkyl interactions. All interactions are hydrophobic, except for conventional hydrogen bonds. The MK-3207 shows strong interactions with the amino acid residues SER72, ALA328, TYR382, and HIS438 in 1P0I. In particular, TYR382 of 1P0I forms multiple interactions (Pi-Pi stacked, alkyl) with the benzene ring in MK-3207. Similarly, SER72 forms a conventional hydrogen bond with a benzene ring in MK-3207. That is, cooperative binding is noted in this case. Our earlier study has mentioned that cooperativity plays an important role in determining the stability of the biomolecular system [58]. The BIOVIA Discovery Studio tool is used in this investigation to examine interaction residues and binding processes.

Table 2. Best poses binding energies (kcal/mol) of Atogepant, Rimegepant, Ubrogapant, MK-3207, Rivastigmine, Galantamine, and Donepezil against 7E3D and 1P0I.

Compounds	7E3D			1P0I		
	Pose – 1	Pose – 2	Pose – 3	Pose – 1	Pose – 2	Pose – 3
Atogepant	-9.8	-9.6	-9.3	-11.9	-11.3	-11.2
Rimegepant	-11.7	-11.2	-11.2	-12.0	-11.6	-11.6
Ubrogapant	-9.6	-9.0	-9.0	-11.2	-10.6	-10.4
MK-3207	-10.6	-10.1	-10.0	-12.1	-11.9	-11.7
Rivastigmine	-6.9	-6.7	-6.7	-7.4	-7.1	-7.0
Galantamine	-7.0	-6.7	-6.4	-8.6	-8.5	-8.4
Donepezil	-9.2	-8.8	-8.8	-9.7	-9.2	-9.2

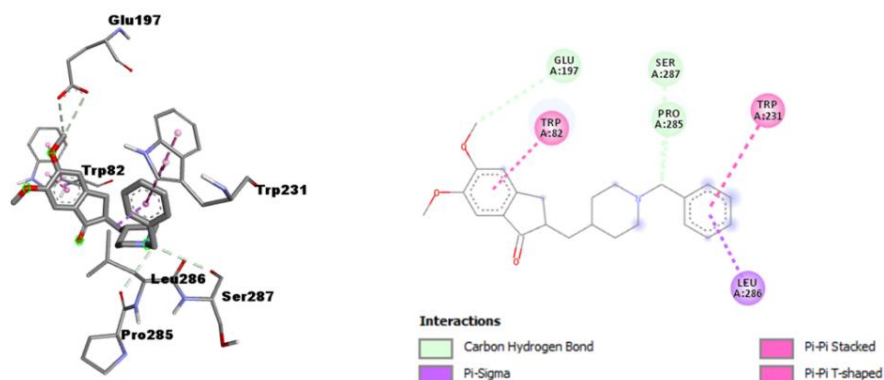
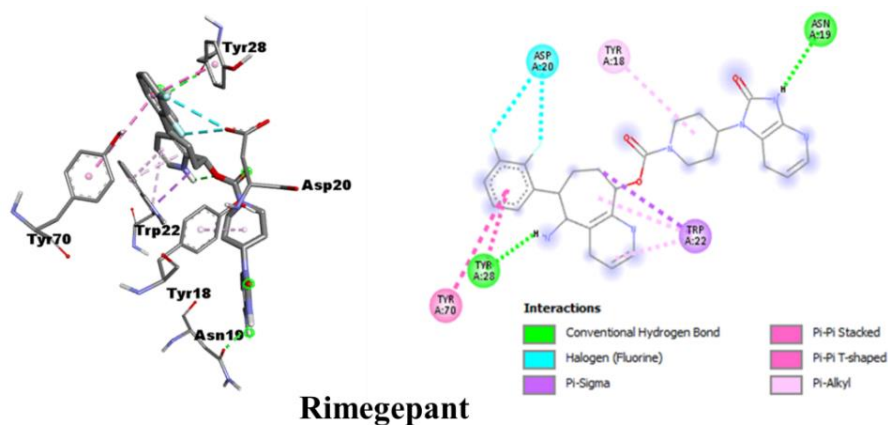


Figure 5. Best docking pose and its 3D (left) and 2D (right) interactions of 7E3D with Rimegepant and Donepezil.

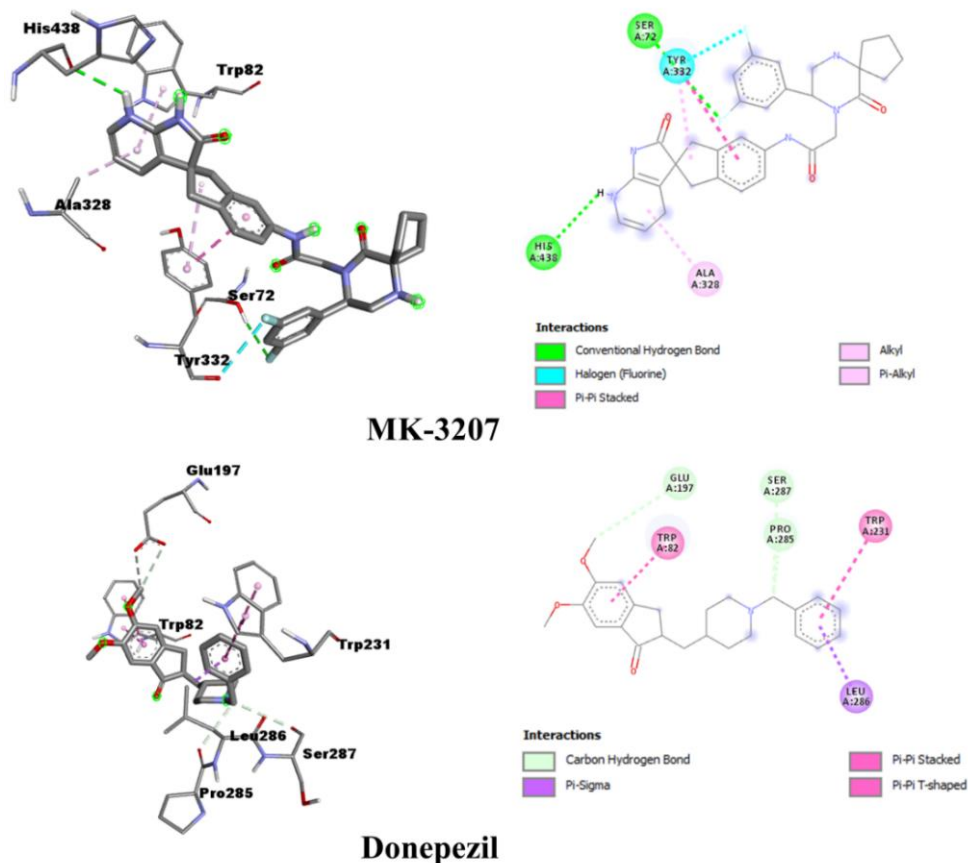


Figure 6. Best docking pose and its 3D (left) and 2D (right) interactions of 1P0I with MK-3207 and Donepezil.

In the case of AD drug molecules, donepezil shows strong interaction with 7E3D and 1P0I. The binding energy of the best pose of donepezil with 7E3D is -9.2 kcal/mol, with 1P0I is -9.7 kcal/mol. Our result coincides well with the earlier study by Ghosh *et al.* They have studied cholinergic inhibition of Alzheimer's disease using donepezil in metadynamics simulations [59,60]. Compared with 7E3D and 1P0I, donepezil shows a stronger interaction with the latter. The reason is that Pi-Pi stacked, Pi-sigma, and Carbon-hydrogen bond interactions occur between 1P0I and donepezil. All the interactions are hydrophobic in nature. While comparing gepant and AD drug molecules' interactions with 7E3D or 1P0I, gepant derivatives, in particular, rimegepant and MK-3207, show strong interaction with 7E3D and 1P0I, respectively. This is due to cooperative binding noted between gepant derivatives with 7E3D and 1P0I. Further, earlier molecular docking studies indicate that the presence of a number of hydrogen bonds influences the binding affinity of the ligand-receptor interaction [61,62].

Numerous compounds possessing carbamate functional groups have been thoroughly examined for their anticholinesterase properties [63,64]. Among them, rivastigmine is the only compound that is used clinically in the management of AD. Among the studied gepant ligands, the carbamate group is available in rimegepant. In summary, both rimegepant and MK-3207 bind strongly to the active sites in 7E3D and 1P0I, respectively. However, three gepant derivatives show similar results in case 1P0I. Hence, a more detailed study is required to get a clear conclusion in this case.

3.5. Molecular dynamics.

To understand the inhibition mechanism in a real-time environment, a molecular dynamics simulation was performed in this study. Molecular dynamics simulation is a more powerful computational method, more effective than docking, and requires less processing. It delivers high precision, capable of providing insights into complex system behavior that experimental methods may not. Molecular dynamics simulations are performed for all gepant derivatives with AChE (7E3D) and BuChE (1P0I). Earlier, Leung *et al.* studied the binding interactions between ubrogepant and rimegepant with calcitonin-gene-related peptide receptor (CGRPR) using MD simulations.

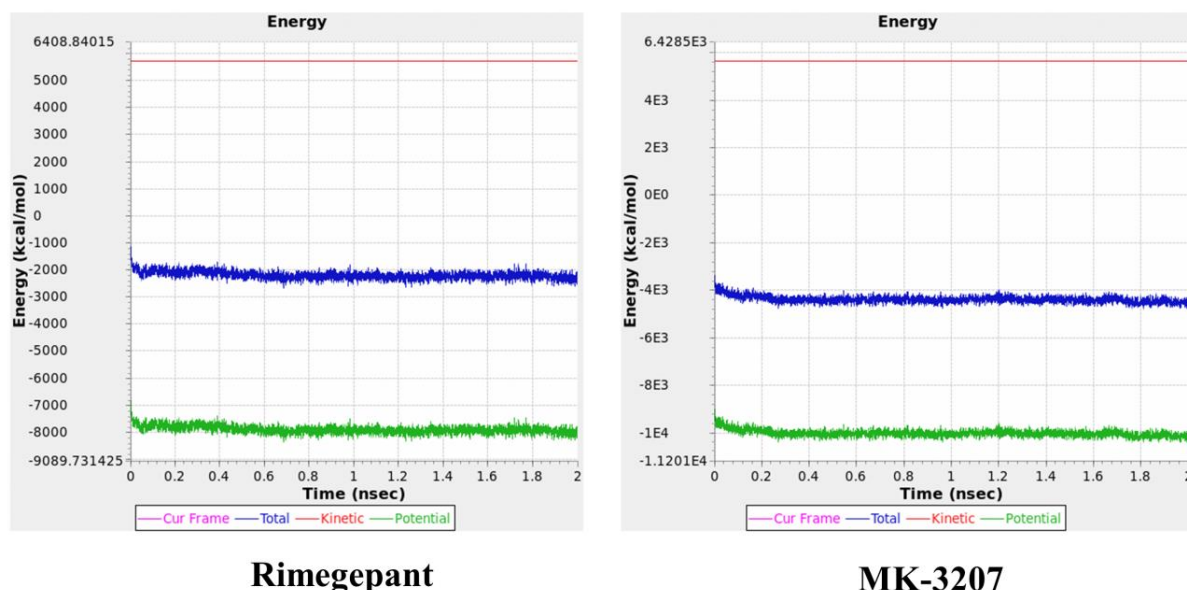


Figure 7. The energy plot of 7E3D with Rimegepant and 1P0I with MK-3207 during the simulation.

They found that ubrogepant binds more strongly with CGRPR than rimegepant due to electrostatic and hydrophobic interactions [65]. The energy plots for 7E3D with rimegepant and 1P0I with MK-3207 are shown in Figure 7. All other energy plots are given in Figure S3 in the supporting information file. The molecular dynamics simulations are performed to understand the stability of selected ligands and receptors [66,67]. In particular, one can examine the stability and structural changes in ligand-receptor complexes using an energy plot. Further, less fluctuation shows the higher stability of the ligand-receptor complex. Our molecular dynamics study reveals less fluctuation in the studied ligand-receptor complex during simulation (Figure 7). That is, the total energy varies between -2800 kcal/mol and -2200 kcal/mol. This indicates that the studied ligand-receptor complex has reached a stable state, implying that the selected ligand interacts well with the 7E3D and 1P0I. The stable state of the ligand-receptor is reached within 0.1 ns.

4. Conclusions

In this study, the migraine drugs, i.e., gepant derivatives, are investigated for their potential anti-Alzheimer activity. The binding mechanisms of the selected gepant derivatives are evaluated against AChE and BuChE using computational techniques, including quantum chemistry, molecular docking, and dynamics studies. The global reactivity descriptors of the molecule have been used to identify reactive sites. The reactive sites, such as electrophilic and nucleophilic centers, of the selected gepant derivatives are identified using quantum-chemical calculations. Our docking study revealed that among the selected gepant derivatives, rimegepant and MK-3207 are active compounds with strong binding energies against AChE and BuChE, respectively. These compounds are good inhibitors of AChE and BuChE, respectively. Therefore, based on our *in silico* studies, rimegepant and MK-3207 are proposed as good candidate molecules for the design of a new drug against AD. Molecular dynamics simulations indicate that it has a stable conformation and aligns with the target protein, suggesting its potential as an anti-Alzheimer's drug. This study reveals that rimegepant and MK-3207, an aromatic molecule with high structural stability and binding energy, could be potential treatments for Alzheimer's disease due to their strong anti-Alzheimer effects. The findings of the current study support the potential of these compounds as effective lead therapeutics for AD, which may aid medical and pharmaceutical chemists in developing and synthesizing more potent medication candidates. It is hoped that the current study's findings will offer important insights for the development of anti-Alzheimer drugs. In summary, the article's goals are to introduce new therapy options that could completely transform patient care and to advance our understanding of AD pathophysiology.

Author Contributions

Karthikeyan Asokan and Selarengan Paranthaman performed and designed the research study. Mahendiraprabhu Ganesan contributed essential tools and analyzed the data. Abiram Angamuthu performed validation and editing. Karthikeyan Asokan and Selarengan Paranthaman wrote the paper.

Institutional Review Board Statement

Not applicable.

Informed Consent Statement

Not applicable.

Data Availability Statement

No new data were created or analyzed in this study. Data sharing is not applicable.

Funding

This research received no external funding.

Acknowledgments

K.A. is thankful to the management of Kalasalingam Academy of Research and Education for the University Research Fellowship. K. A. and S.P. are grateful to Prof. Milton Franklin Benial A, Department of Physics, N.M.S.S.Vellaichamy Nadar College, Madurai, for the GaussView5 program.

Conflicts of Interest

The authors declare no conflict of interest.

Abbreviation

The following abbreviations are used in this manuscript:

Abbreviation	Definition
AD	Alzheimer's Disease
WHO	World Health Organization
GSK3	Glycogen Synthase Kinase 3
BACE1	β -Secretase
MAO	Monoamine Oxidase
AChE	Acetylcholinesterase
BuChE	Butyrylcholinesterase
ACh	Acetylcholine
FDA	Food and Drug Administration
DFT	Density Functional Theory
FMO	Frontier Molecular Orbital
HOMO	Highest Occupied Molecular Orbital
LUMO	Lowest Unoccupied Molecular Orbital
MEP	Molecular Electrostatic Potential
MD	Molecular Dynamics
CGRPR	Calcitonin-Gene Related Peptide Receptor
NFL	Neurofilament Light Chain
PDB	Protein Data Bank

References

1. Hiremathad, A.; Keri, R. S.; Esteves, A. R.; Cardoso, S. M.; Chaves, S.; Santos, M. A. Novel Tacrine-Hydroxyphenylbenzimidazole Hybrids as Potential Multitarget Drug Candidates for Alzheimer's Disease. *Eur. J. Med. Chem.* **2018**, *148*, 255–267, <https://doi.org/10.1016/j.ejmech.2018.02.023>.

2. Sharma, A.; Pachauri, V.; Flora, S. J. S. Advances in Multi-Functional Ligands and the Need for Metal-Related Pharmacology for the Management of Alzheimer Disease. *Front. Pharmacol.* **2018**, *9*, 1–19, <https://doi.org/10.3389/fphar.2018.01247>.
3. Tzioras, M.; McGeachan, R. I.; Durrant, C. S.; Spires-Jones, T. L. Synaptic Degeneration in Alzheimer Disease. *Nat. Rev. Neurol.* **2023**, *19*, 19–38, <https://doi.org/10.1038/s41582-022-00749-z>.
4. Goedert, M.; Spillantini, M. G. A Century of Alzheimer's Disease. *Science* **2006**, *314*, 777–781, <https://doi.org/10.1126/science.1132814>.
5. van der Flier, W. M.; de Vugt, M. E.; Smets, E. M. A.; Blom, M.; Teunissen, C. E. Towards a Future Where Alzheimer's Disease Pathology Is Stopped before the Onset of Dementia. *Nat. Aging* **2023**, *3*, 494–505, <https://doi.org/10.1038/s43587-023-00404-2>.
6. Rizzo, M. G.; De Plano, L. M.; Palermo, N.; Franco, D.; Nicolò, M.; Sciuto, E. L.; Calabrese, G.; Oddo, S.; Conoci, S.; Guglielmino, S. P. P. A Novel Serum-Based Diagnosis of Alzheimer's Disease Using an Advanced Phage-Based Biochip. *Adv. Sci.* **2023**, *10*, 2301650, <https://doi.org/10.1002/advs.202301650>.
7. Hooper, C.; Killick, R.; Lovestone, S. The GSK3 Hypothesis of Alzheimer's Disease. *J. Neurochem.* **2008**, *104*, 1433–1439. <https://doi.org/10.1111/j.1471-4159.2007.05194.x>.
8. Sequeira, R.C.; Godad, A. Understanding Glycogen Synthase Kinase-3: A Novel Avenue for Alzheimer's Disease. *Mol. Neurobiol.* **2023**, *61*, 4203–4221, <https://doi.org/10.1007/s12035-023-03839-1>.
9. Shahrivar-Gargari, M.; Hamzeh-Mivehroud, M.; Hemmati, S.; Shahbazi Mojarrad, J.; Notash, B.; Tüylü Küçükılınç, T.; Ayazgök, B.; Dastmalchi, S. Design, Synthesis, and Biological Evaluation of Novel Indanone-Based Hybrids as Multifunctional Cholinesterase Inhibitors for Alzheimer's Disease. *J. Mol. Struct.* **2021**, *1229*, 129787, <https://doi.org/10.1016/j.molstruc.2020.129787>.
10. Baracaldo-Santamaría, D.; Avendaño-Lopez, S.S.; Ariza-Salamanca, D.F.; Rodriguez-Giraldo, M.; Calderon-Ospina, C.A.; González-Reyes, R.E.; Nava-Mesa, M.O. Role of Calcium Modulation in the Pathophysiology and Treatment of Alzheimer's Disease. *Int. J. Mol. Sci.* **2023**, *24*, 9067, <https://doi.org/10.3390/ijms24109067>.
11. Ionescu-Tucker, A.; Cotman, C.W. Emerging roles of oxidative stress in brain aging and Alzheimer's disease. *Neurobiol. Aging* **2021**, *107*, 86–95, <https://doi.org/10.1016/j.neurobiolaging.2021.07.014>.
12. Bai, R.; Guo, J.; Ye, X.-Y.; Xie, Y.; Xie, T. Oxidative Stress: The Core Pathogenesis and Mechanism of Alzheimer's Disease. *Ageing Res. Rev.* **2022**, *77*, 101619, <https://doi.org/10.1016/j.arr.2022.101619>.
13. Swerdlow, R.H. Mitochondria and Mitochondrial Cascades in Alzheimer's Disease. *J. Alzheimer's Dis.* **2018**, *62*, 1403–1416, <https://doi.org/10.3233/JAD-170585>.
14. Fišar, Z. Linking the Amyloid, Tau, and Mitochondrial Hypotheses of Alzheimer's Disease and Identifying Promising Drug Targets. *Biomolecules* **2022**, *12*, 1676, <https://doi.org/10.3390/biom12111676>.
15. Yamazaki, Y.; Zhao, N.; Caulfield, T.R.; Liu, C.C.; Bu, G. Apolipoprotein E and Alzheimer Disease: Pathobiology and Targeting Strategies. *Nat. Rev. Neurol.* **2019**, *15*, 501–518, <https://doi.org/10.1038/s41582-019-0228-7>.
16. Moussa-Pacha, N.M.; Abdin, S.M.; Omar, H.A.; Alniss, H.; Al-Tel, T.H. BACE1 Inhibitors: Current Status and Future Directions in Treating Alzheimer's Disease. *Med. Res. Rev.* **2020**, *40*, 339–384, <https://doi.org/10.1002/med.21622>.
17. Bazzari, F.H.; Bazzari, A.H. BACE1 Inhibitors for Alzheimer's Disease: The Past, Present and Any Future? *Molecules* **2022**, *27*, 8823, <https://doi.org/10.3390/molecules27248823>.
18. Riederer, P.; Danielczyk, W.; Grünblatt, E. Monoamine Oxidase-B Inhibition in Alzheimer's Disease. *Neurotoxicology* **2004**, *25*, 271–277, [https://doi.org/10.1016/S0161-813X\(03\)00106-2](https://doi.org/10.1016/S0161-813X(03)00106-2).
19. Bhawna; Kumar, A.; Bhatia, M.; Kapoor, A.; Kumar, P.; Kumar, S. Monoamine Oxidase Inhibitors: A Concise Review with Special Emphasis on Structure Activity Relationship Studies. *Eur. J. Med. Chem.* **2022**, *242*, 114655, <https://doi.org/10.1016/j.ejmech.2022.114655>.
20. Wang, L.; Yin, Y.-L.; Liu, X.-Z.; Shen, P.; Zheng, Y.-G.; Lan, X.-R.; Lu, C.-B.; Wang, J.-Z. Current Understanding of Metal Ions in the Pathogenesis of Alzheimer's Disease. *Transl. Neurodegener.* **2020**, *9*, 10, <https://doi.org/10.1186/s40035-020-00189-z>.
21. Zafar, R.; Zubair, M.; Ali, S.; Shahid, K.; Waseem, W.; Naureen, H.; Haider, A.; Jan, M. S.; Ullah, F.; Sirajuddin, M.; Sadiq, A. Zinc Metal Carboxylates as Potential Anti-Alzheimer's Candidate: In Vitro Anticholinesterase, Antioxidant and Molecular Docking Studies. *J. Biomol. Struct. Dyn.* **2021**, *39*, 1044–1054, <https://doi.org/10.1080/07391102.2020.1724569>.

22. Martins, M.M.; Branco, P.S.; Ferreira, L.M. Enhancing the Therapeutic Effect in Alzheimer's Disease Drugs: The Role of Polypharmacology and Cholinesterase Inhibitors. *ChemistrySelect* **2023**, *8*, e202300461, <https://doi.org/10.1002/slct.202300461>.
23. Gargari, M.S.; Mivehroud, M.H.; Hemmati, S.; Mojarrad, J.S.; Tüylü, T.; Ayazgök, B. Hybridization - Based Design of Novel Anticholinesterase Indanone – Carbamates for Alzheimer's Disease: Synthesis, Biological Evaluation, and Docking Studies. *Arch. Pharm.* **2021**, *354*, 2000453, <https://doi.org/10.1002/ardp.202000453>.
24. Abdallah, A.E. Review on Anti-Alzheimer Drug Development: Approaches, Challenges and Perspectives. *RSC Adv.* **2024**, *14*, 11057–11088, <https://doi.org/10.1039/d3ra08333k>.
25. Lahiri, D.K.; Farlow, M.R.; Greig, N.H.; Sambamurti, K. Current Drug Targets for Alzheimer's Disease Treatment. *Drug Dev. Res.* **2002**, *56*, 267–281, <https://doi.org/10.1002/ddr.10081>.
26. Taléns-Visconti, R.; de Julián-Ortiz, J. V.; Vila-Busó, O.; Diez-Sales, O.; Nacher, A. Intranasal Drug Administration in Alzheimer-Type Dementia: Towards Clinical Applications. *Pharmaceutics* **2023**, *15*, 1399 <https://doi.org/10.3390/pharmaceutics15051399>.
27. Yasir Hasan Siddique Falaq Naz, R.H.V.M.I.; Shahid, M. Effect of Donepezil Hydrochloride on the Transgenic Drosophila Expressing Human A β -42. *Int. J. Neurosci.* **2023**, *134*, 1293-1308, <https://doi.org/10.1080/00207454.2023.2262109>.
28. Benninghoff, J.; Perneczky, R. Anti-Dementia Medications and Anti-Alzheimer's Disease Drugs: Side Effects, Contraindications, and Interactions. In *NeuroPsychopharmacotherapy*, Riederer, P., Laux, G., Nagatsu, T., Le, W., Riederer, C., Eds.; Springer International Publishing: Cham, **2020**; pp. 1-10, https://doi.org/10.1007/978-3-319-56015-1_195-1.
29. Pushpakom, S.; Iorio, F.; Eyers, P.A.; Escott, K.J.; Hopper, S.; Wells, A.; Doig, A.; Guilliams, T.; Latimer, J.; McNamee, C.; Norris, A.; Sanseau, P.; Cavalla, D.; Pirmohamed, M. Drug Repurposing: Progress, Challenges and Recommendations. *Nat. Rev. Drug Discov.* **2018**, *18*, 41–58, <https://doi.org/10.1038/nrd.2018.168>.
30. Parvathaneni, V.; Kulkarni, N.S.; Muth, A.; Gupta, V. Drug Repurposing: A Promising Tool to Accelerate the Drug Discovery Process. *Drug Discov. Today* **2019**, *24*, 2076–2085, <https://doi.org/10.1016/j.drudis.2019.06.014>.
31. Alhakamy, N.A.; Md, S. Repurposing Itraconazole Loaded PLGA Nanoparticles for Improved Antitumor Efficacy in Non-Small Cell Lung Cancers. *Pharmaceutics* **2019**, *11*, 685, <https://doi.org/10.3390/pharmaceutics11120685>.
32. Doumat, G.; Daher, D.; Zerdan, M.B.; Nasra, N.; Bahmad, H.F.; Recine, M.; Poppiti, R. Drug Repurposing in Non-Small Cell Lung Carcinoma: Old Solutions for New Problems. *Curr. Oncol.* **2023**, *30*, 704–719, <https://doi.org/10.3390/curroncol30010055>.
33. Kabir, E.R.; Siami, M.K.S.; Kabir, S.M.; Khan, A.; Rajib, S.A. Drug Repurposing: Targeting MTOR Inhibitors for Anticancer Activity. *ACM Int. Conf. Proceeding Ser.* **2017**, 68–75, <https://doi.org/10.1145/3156346.3156359>.
34. Mohi-ud-din, R.; Chawla, A.; Sharma, P.; Mir, P.A.; Potoo, F.H.; Reiner, Ž.; Reiner, I.; Ateşşahin, D.A.; Sharifi-Rad, J.; Mir, R.H.; Calina, D. Repurposing Approved Non-Oncology Drugs for Cancer Therapy: A Comprehensive Review of Mechanisms, Efficacy, and Clinical Prospects. *Eur. J. Med. Res.* **2023**, *28*, 345, <https://doi.org/10.1186/s40001-023-01275-4>.
35. Rajasekhar, K.; Chakrabarti, M.; Govindaraju, T. Function and Toxicity of Amyloid Beta and Recent Therapeutic Interventions Targeting Amyloid Beta in Alzheimer's Disease. *Chem. Commun.* **2015**, *51*, 13434-13450, <https://doi.org/10.1039/C5CC05264E>.
36. Jouanne, M.; Rault, S.; Voisin-Chiret, A.-S. Tau Protein Aggregation in Alzheimer's Disease: An Attractive Target for the Development of Novel Therapeutic Agents. *Eur. J. Med. Chem.* **2017**, *139*, 153–167, <https://doi.org/10.1016/j.ejmech.2017.07.070>.
37. Panza, F.; Lozupone, M. The Challenges of Anti-Tau Therapeutics in Alzheimer Disease. *Nat. Rev. Neurol.* **2022**, *18*, 577–578, <https://doi.org/10.1038/s41582-022-00702-0>.
38. Marucci, G.; Buccioni, M.; Dal Ben, D.; Lambertucci, C.; Volpini, R.; Amenta, F. Efficacy of Acetylcholinesterase Inhibitors in Alzheimer's Disease. *Neuropharmacology* **2021**, *190*, 108352, <https://doi.org/10.1016/j.neuropharm.2020.108352>.
39. Morton, R.E.; St. John, P.D.; Tyas, S.L. Migraine and the Risk of All-Cause Dementia, Alzheimer's Disease, and Vascular Dementia: A Prospective Cohort Study in Community-Dwelling Older Adults. *Int. J. Geriatr. Psychiatry* **2019**, *34*, 1667–1676, <https://doi.org/10.1002/gps.5180>.

40. Avgoustou, P.; Jailani, A.B.A.; Zirimwabagabo, J.O.; Tozer, M.J.; Gibson, K.R.; Glossop, P.A.; Mills, J. E.J.; Porter, R.A.; Blaney, P.; Bungay, P.J.; Wang, N.; Shaw, A.P.; Bigos, K.J.A.; Holmes, J.L.; Warrington, J.I.; Skerry, T.M.; Harrity, J.P.A.; Richards, G.O. Discovery of a First-in-Class Potent Small Molecule Antagonist against the Adrenomedullin-2 Receptor. *ACS Pharmacol. Transl. Sci.* **2020**, *3*, 706–719, <https://doi.org/10.1021/acspsci.0c00032>.
41. Sangalli, L.; Brazzoli, S. Calcitonin Gene-Related Peptide (CGRP)-Targeted Treatments—New Therapeutic Technologies for Migraine. *Futur. Pharmacol.* **2023**, *3*, 117–131, <https://doi.org/10.3390/futurepharmacol3010008>.
42. Pleş, H.; Florian, I.-A.; Timis, T.-L.; Covache-Busuioac, R.-A.; Glavan, L.-A.; Dumitrascu, D.-I.; Popa, A. A.; Bordeianu, A.; Ciurea, A. V. Migraine: Advances in the Pathogenesis and Treatment. *Neurol. Int.* **2023**, *15*, 1052–1105, <https://doi.org/10.3390/neurolint15030067>.
43. Becke, A.D. Density-Functional Exchange-Energy Approximation with Correct Asymptotic Behavior. *Phys. Rev. A* **1988**, *38*, 3098–3100, <https://doi.org/10.1103/PhysRevA.38.3098>.
44. Lee, C.; Yang, W.; Parr, R. G. Development of the Colle-Salvetti Correlation-Energy Formula into a Functional of the Electron Density. *Phys. Rev. B* **1988**, *37*, 785–789, <https://doi.org/10.1103/PhysRevB.37.785>.
45. Dennington, R.; Keith, T.; Millam, J.; GaussView, Version 5. Semichem Inc., Shawnee Mission, **2009**.
46. Frisch, M.J.; Trucks, G.; Schlegel, H.B.; Scuseria, G.E.; Robb, M.A.; Cheeseman, J.R.; Scalmani, G.; Barone, V.; Mennucci, B.; Petersson, G.A.; Nakatsuji, h.; Caricato, M.; Li, X.; Hratchian, H.P.; Izmaylov, A.F.; Bloino, J.; Zheng, G.; Sonnenberg, J.L.; Hada, M.; Ehara, M.; Toyota, K.; Fukuda, R.; Hasegawa, J.; Ishida, M.; Nakajima, T.; Honda, Y.; Kitao, O.; Nakai, H.; Vreven, T.; Montgomery, J.; Peralta, J.E.; Ogliaro, F.; Bearpark, M.; Heyd, J.J.; Brothers, E.; Kudin, K.N.; Staroverov, V.N.; Kobayashi, R.; Normand, J.; Raghavachari, K.; Rendell, A.P.; Burant, J.C.; Iyengar, S.S.; Tomasi, J.; Cossi, M.; Rega, N.; Millam, J.M.; Klene, M.; Knoq, J.E.; Cross, J.B.; Bakken, V.; Adamo, C.; Jaramillo, J.; Gomperts, R.; Stratmann, R.E.; Yazyev, O.; Austin, A.J.; Cammi, R.; Pomelli, C.S.; Ochterski, J.W.; Martin, R.L.; Morokuma, K.; Zakrzewski, V.G.; Voth, G.A.; Salvador, P.; Dannenberg, J.J.; Dapprich, S.; Daniels, A.D.; Farkas, F.J.B.; Ortiz, J.V.; Cioslowski, J.; Fox, D.J. Gaussian 09 Revision A.1. Gaussian Inc, **2009**.
47. Dallakyan, S.; Olson, A.J. Small-Molecule Library Screening by Docking with PyRx. In *Chemical Biology: Methods and Protocols*, Hempel, J.E., Williams, C.H., Hong, C.C., Eds.; Springer New York: New York, NY, **2015**; Volume 1263, pp. 243-250, https://doi.org/10.1007/978-1-4939-2269-7_19.
48. Biovia, D.S. Discovery Studio Modeling Environment. *Release* **2017**.
49. Fukunishi, Y.; Mikami, Y.; Nakamura, H. The Filling Potential Method: A Method for Estimating the Free Energy Surface for Protein–Ligand Docking. *J. Phys. Chem. B* **2003**, *107*, 13201–13210, <https://doi.org/10.1021/jp035478e>.
50. Elangovan, N.D.; Dhanabalan, A.K.; Gunasekaran, K.; Kandimalla, R.; Sankarganesh, D. Screening of Potential Drug for Alzheimer’s Disease: A Computational Study with GSK-3 β Inhibition through Virtual Screening, Docking, and Molecular Dynamics Simulation. *J. Biomol. Struct. Dyn.* **2021**, *39*, 7065–7079, <https://doi.org/10.1080/07391102.2020.1805362>.
51. Rasul, H.H.; Mamad, D.M.; Azeez, Y.H.; Omer, R.A.; Omer, K.A. Theoretical Investigation on Corrosion Inhibition Efficiency of Some Amino Acid Compounds. *Comput. Theor. Chem.* **2023**, *1225*, 114177, <https://doi.org/10.1016/j.comptc.2023.114177>.
52. Esha, N.J.I.; Quayum, S.T.; Saif, M.Z.; Almatarneh, M.H.; Rahman, S.; Alodhayb, A.; Poirier, R.A.; Uddin, K.M. Exploring the Potential of Fluoro-Flavonoid Derivatives as Anti-Lung Cancer Agents: DFT, Molecular Docking, and Molecular Dynamics Techniques. *Int. J. Quantum Chem.* **2024**, *124*, e27274, <https://doi.org/10.1002/qua.27274>.
53. Pearson, R.G. The Principle of Maximum Hardness. *Acc. Chem. Res.* **1993**, *26*, 250–255, <https://doi.org/10.1021/ar00029a004>.
54. Gadre, S.R.; Shirsat, R.N. *Electrostatics of Atoms and Molecules*. Universities Press: **2000**.
55. Murray, J.S.; Sen, K. *Molecular Electrostatic Potentials: Concepts and Applications*. Elsevier, **1996**; Volume 3.
56. Politzer, P.; Truhlar, D.G. *Chemical Applications of Atomic and Molecular Electrostatic Potentials: Reactivity, Structure, Scattering, and Energetics of Organic, Inorganic, and Biological Systems*; Springer Book Archive: Springer New York, NY, **2013**; <https://doi.org/10.1007/978-1-4757-9634-6>.
57. Kawsar, S.M.A.; Hosen, M.A. An Optimization and Pharmacokinetic Studies of Some Thymidine Derivatives. *Turkish Comput. Theor. Chem.* **2020**, *4*, 59–66, <https://doi.org/10.33435/tcandtc.718807>.

58. Selvarengan, P.; Kolandaivel, P.G. Molecular Modeling of Dipeptide and Its Analogous Systems with Water. *J. Mol. Model.* **2004**, *10*, 198–203, <https://doi.org/10.1007/s00894-004-0184-y>.
59. Ghosh, S.; Jana, K.; Ganguly, B. Revealing the Mechanistic Pathway of Cholinergic Inhibition of Alzheimer's Disease by Donepezil: A Metadynamics Simulation Study. *Phys. Chem. Chem. Phys.* **2019**, *21*, 13578–13589, <https://doi.org/10.1039/c9cp02613d>.
60. Shibaji Ghosh Kalyanashis Jana, P.D.W.; Ganguly, B. Revealing the Cholinergic Inhibition Mechanism of Alzheimer's by Galantamine: A Metadynamics Simulation Study. *J. Biomol. Struct. Dyn.* **2022**, *40*, 5100–5111, <https://doi.org/10.1080/07391102.2020.1867644>.
61. Adeniji, S.E.; Arthur, D.E.; Abdullahi, M.; Haruna, A. Quantitative Structure–Activity Relationship Model, Molecular Docking Simulation and Computational Design of Some Novel Compounds Against DNA Gyrase Receptor. *Chem. Afr.* **2020**, *3*, 391–408, <https://doi.org/10.1007/s42250-020-00132-9>.
62. Duklan, S.; Saha, S.; Jakhmola, V.; Gairola, N.; Pandey, P.; Singh, M.; Kawsar, S.M.A. Molecular Docking, Synthesis, In-Vitro Alpha Amylase and Antibacterial Activities of Newer Generation Pyrimidine Derivatives. *Adv. J. Chem. A.* **2024**, *7*, 459–476, <https://doi.org/10.48309/ajca.2024.448978.1499>.
63. Sang, Z.; Qiang, X.; Li, Y.; Wu, B.; Zhang, H.; Zhao, M.; Deng, Y. Design, Synthesis, and Biological Evaluation of Scutellarein Carbamate Derivatives as Potential Multifunctional Agents for the Treatment of Alzheimer's Disease. *Chem. Biol. Drug Des.* **2015**, *86*, 1168–1177, <https://doi.org/10.1111/cbdd.12580>.
64. Kurt, B.Z.; Gazioglu, I.; Dag, A.; Salmas, R. E.; Kayik, G.; Durdagi, S.; Sonmez, F. Synthesis, Anticholinesterase Activity and Molecular Modeling Study of Novel Carbamate-Substituted Thymol/Carvacrol Derivatives. *Bioorg. Med. Chem.* **2017**, *25*, 1352–1363, <https://doi.org/10.1016/j.bmc.2016.12.037>.
65. Leung, L.; Liao, S.; Wu, C. To Probe the Binding Interactions between Two FDA Approved Migraine Drugs (Ubrogepant and Rimegepant) and Calcitonin-Gene Related Peptide Receptor (CGRPR) Using Molecular Dynamics Simulations. *ACS Chem. Neurosci.* **2021**, *12*, 2629–2642, <https://doi.org/10.1021/acscchemneuro.1c00135>.
66. Suha, H. N.; Hossain, M. S.; Rahman, S.; Alodhayb, A.; Hossain, M. M.; Kawsar, S. M. A.; Poirier, R.; Uddin, K. M. In Silico Discovery and Predictive Modeling of Novel Acetylcholinesterase (AChE) Inhibitors for Alzheimer's Treatment. *Med. Chem.* **2024**, *21*, 345–366, <https://doi.org/10.2174/0115734064304100240511112619>.
67. Kawsar, S.M.A.; Munia, N.S.; Saha, S.; Ozeki, Y. In Silico Pharmacokinetics, Molecular Docking and Molecular Dynamics Simulation Studies of Nucleoside Analogs for Drug Discovery- A Mini Review. *Mini Rev. Med. Chem.* **2024**, *24*, 1070–1088, <https://doi.org/10.2174/0113895575258033231024073521>.

Publisher's Note & Disclaimer

The statements, opinions, and data presented in this publication are solely those of the individual author(s) and contributor(s) and do not necessarily reflect the views of the publisher and/or the editor(s). The publisher and/or the editor(s) disclaim any responsibility for the accuracy, completeness, or reliability of the content. Neither the publisher nor the editor(s) assume any legal liability for any errors, omissions, or consequences arising from the use of the information presented in this publication. Furthermore, the publisher and/or the editor(s) disclaim any liability for any injury, damage, or loss to persons or property that may result from the use of any ideas, methods, instructions, or products mentioned in the content. Readers are encouraged to independently verify any information before relying on it, and the publisher assumes no responsibility for any consequences arising from the use of materials contained in this publication.

Supplementary materials

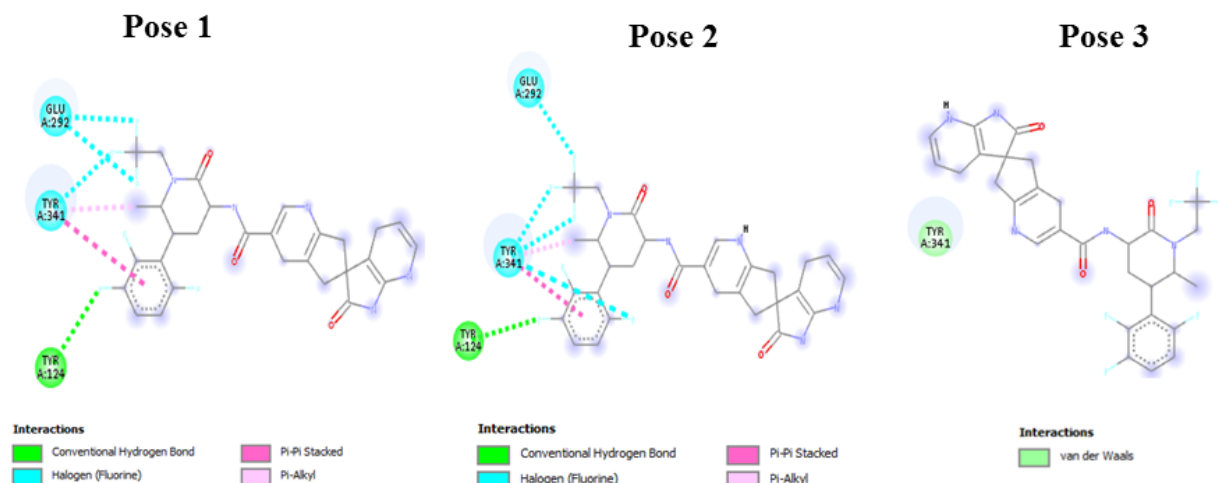


Figure S1. (a) The 2D interactions of the three best possible allosteric binding modes (poses) of the Atogepant ligand with AChE (7E3D).

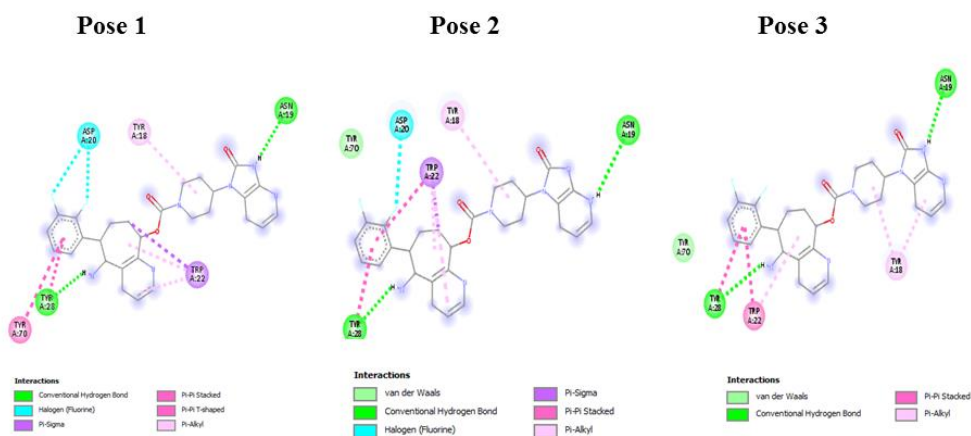


Figure S1. (b) The 2D interactions of the three best possible allosteric binding modes (poses) of the Rimegepant ligand with AChE (7E3D).

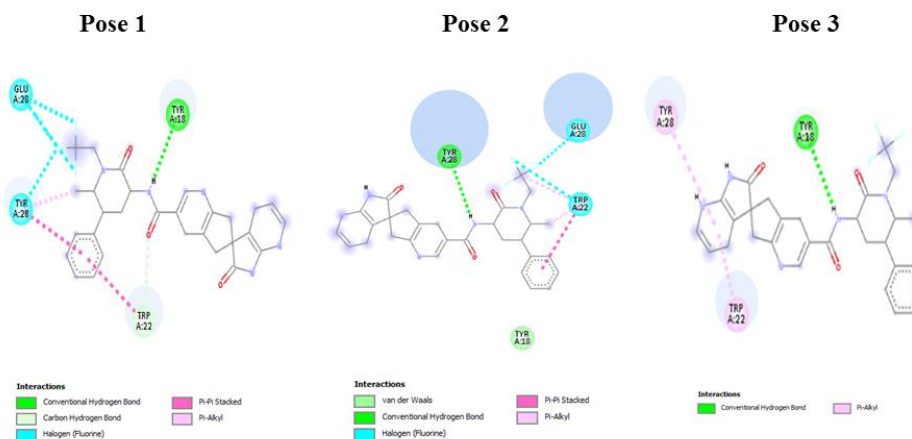


Figure S1. (c) The 2D interactions of the three best possible allosteric binding modes (poses) of the Ubrogapant ligand with AChE (7E3D).

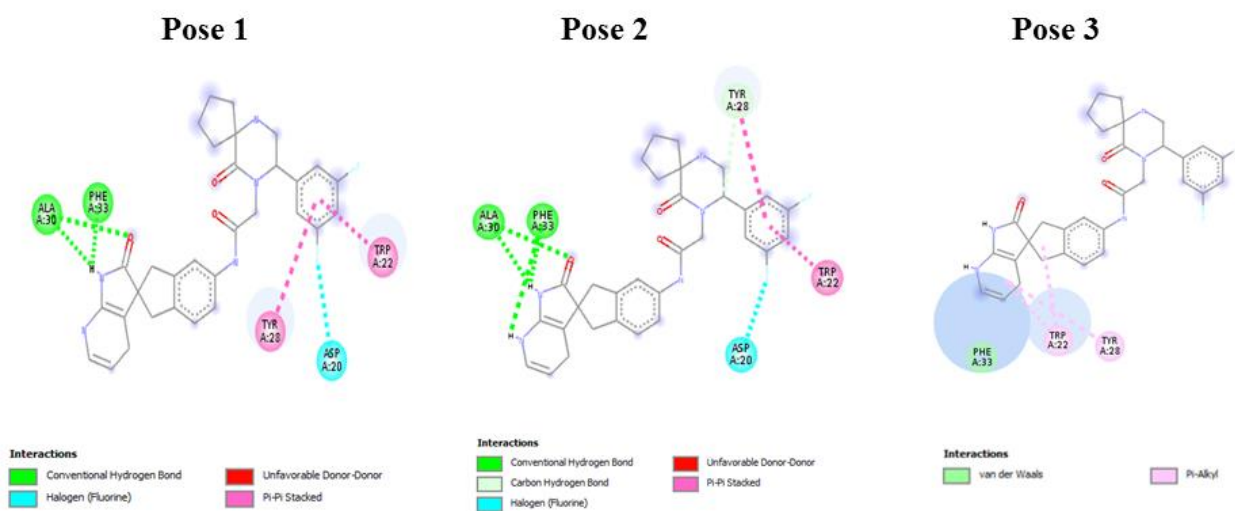


Figure S1. (d) The 2D interactions of the three best possible allosteric binding modes (poses) of the MK-3207 ligand with AChE (7E3D).

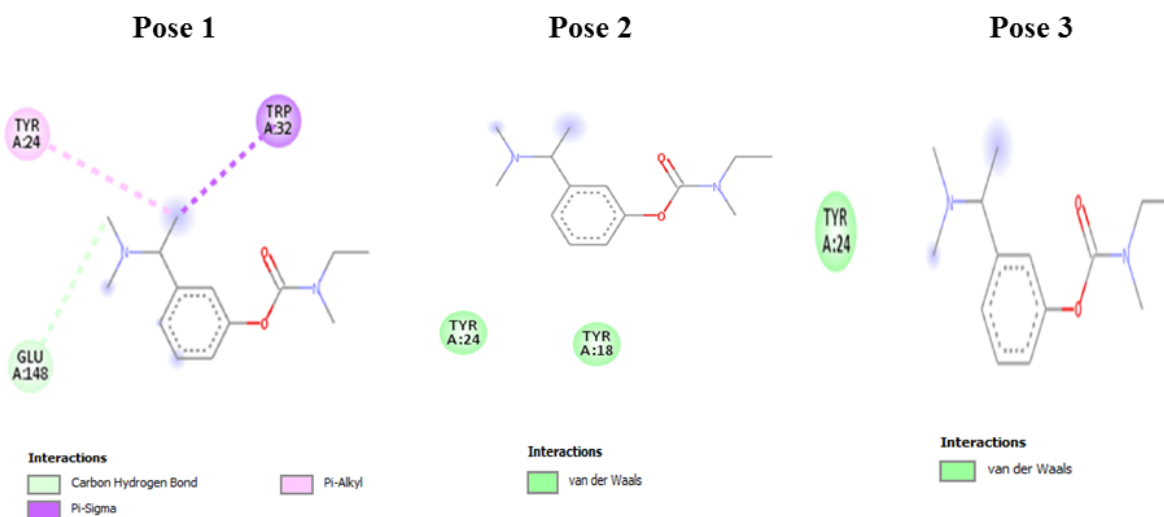


Figure S1. (e) The 2D interactions of the three best possible allosteric binding modes (poses) of the Rivastigmine (77991) ligand with AChE (7E3D).

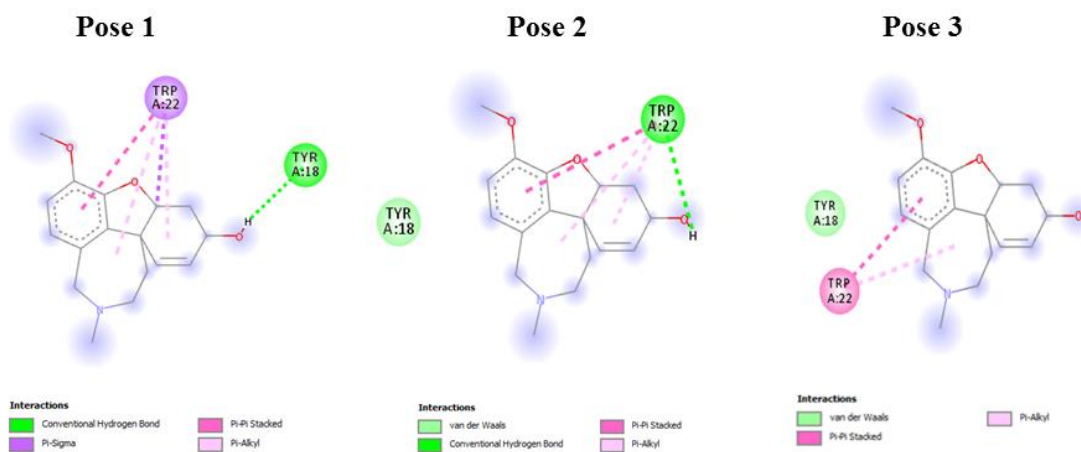


Figure S1. (f) The 2D interactions of the three best possible allosteric binding modes (poses) of the Galantamine (9651) ligand with AChE (7E3D).

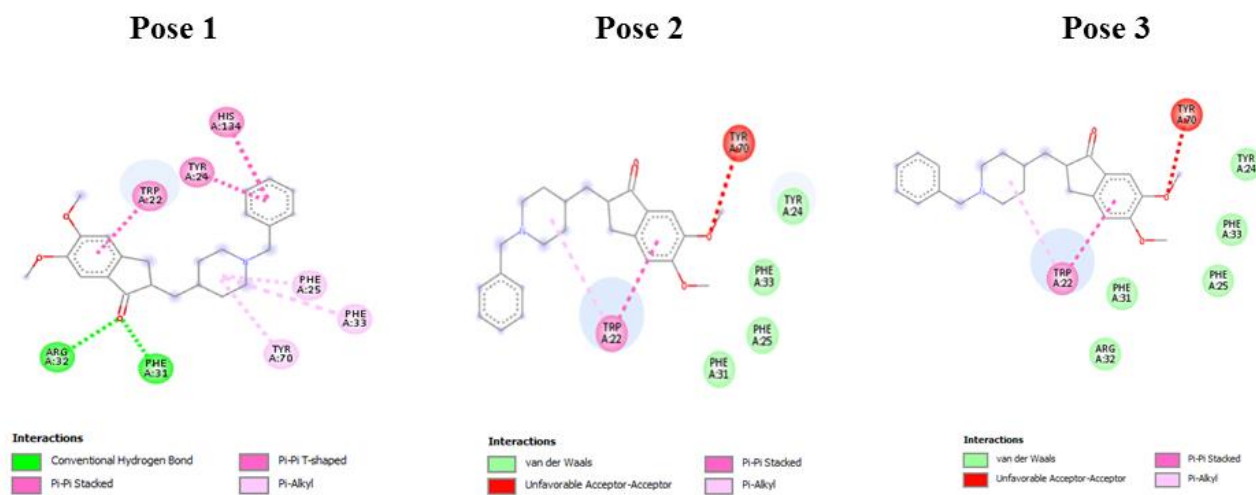


Figure S1. (g) The 2D interactions of the three best possible allosteric binding modes (poses) of the Donepezil (3152) ligand with AChE (7E3D).

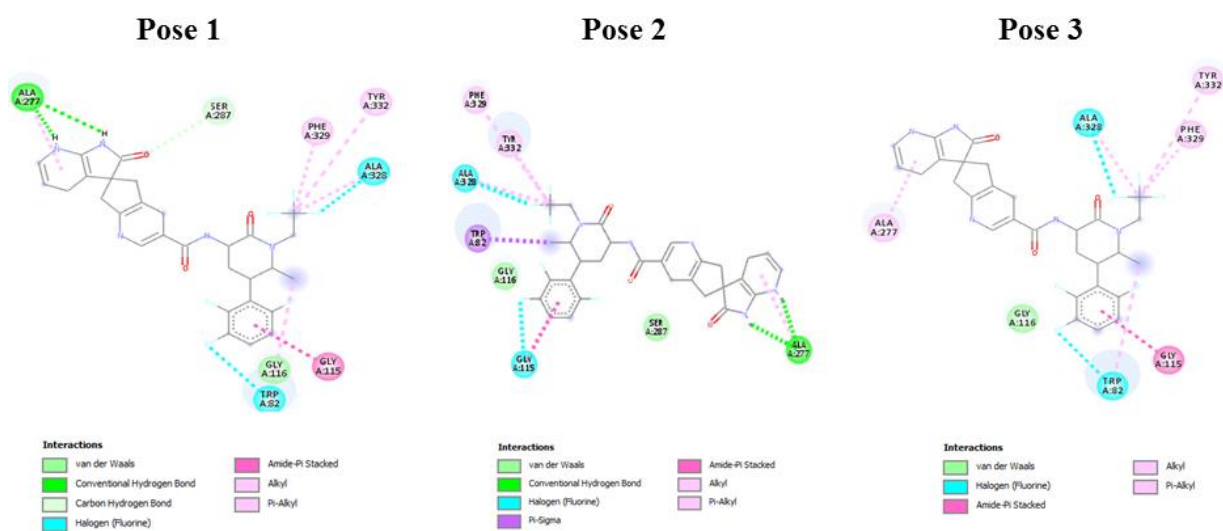


Figure S2. (a) The 2D interactions of the three best possible allosteric binding modes (poses) of the Atogepant ligand with BuChE (1P0D).

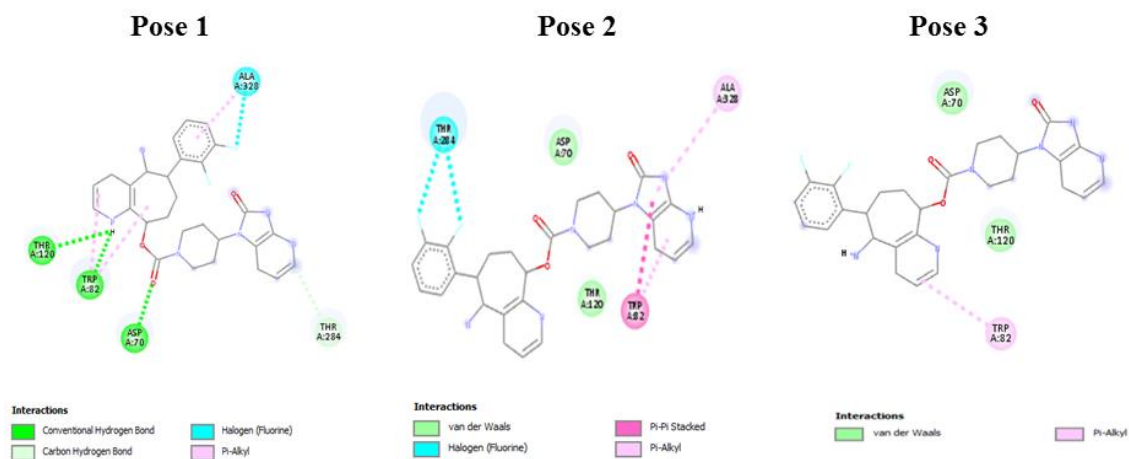


Figure S2. (b) The 2D interactions of the three best possible allosteric binding modes (poses) of the Rimegepant ligand with BuChE (1P0I).

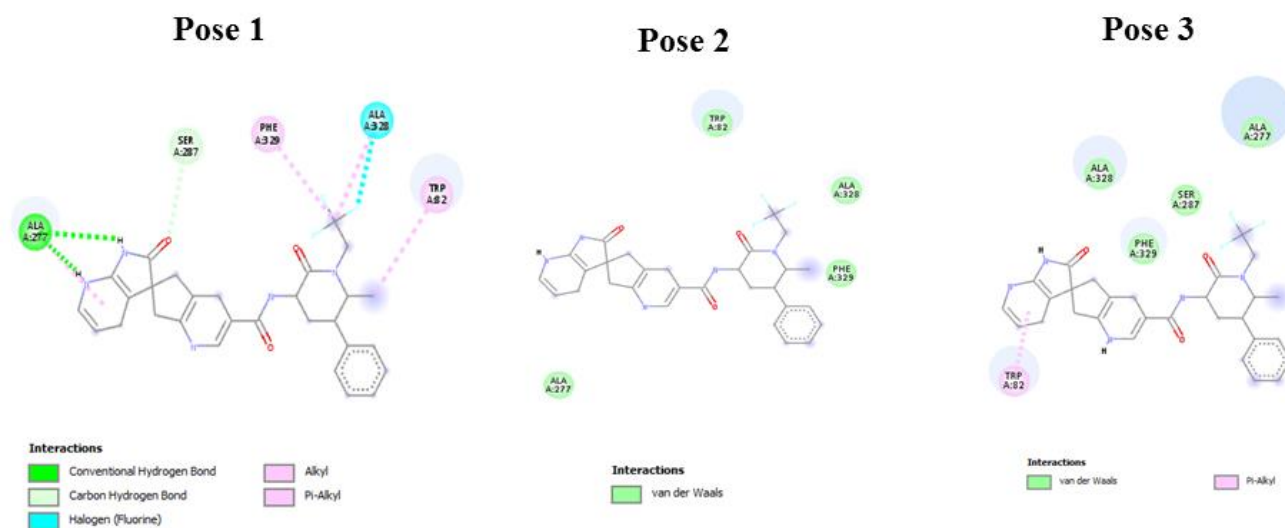


Figure S2. (c) The 2D interactions of the three best possible allosteric binding modes (poses) of the Ubrogепant ligand with BuChE (1POI).

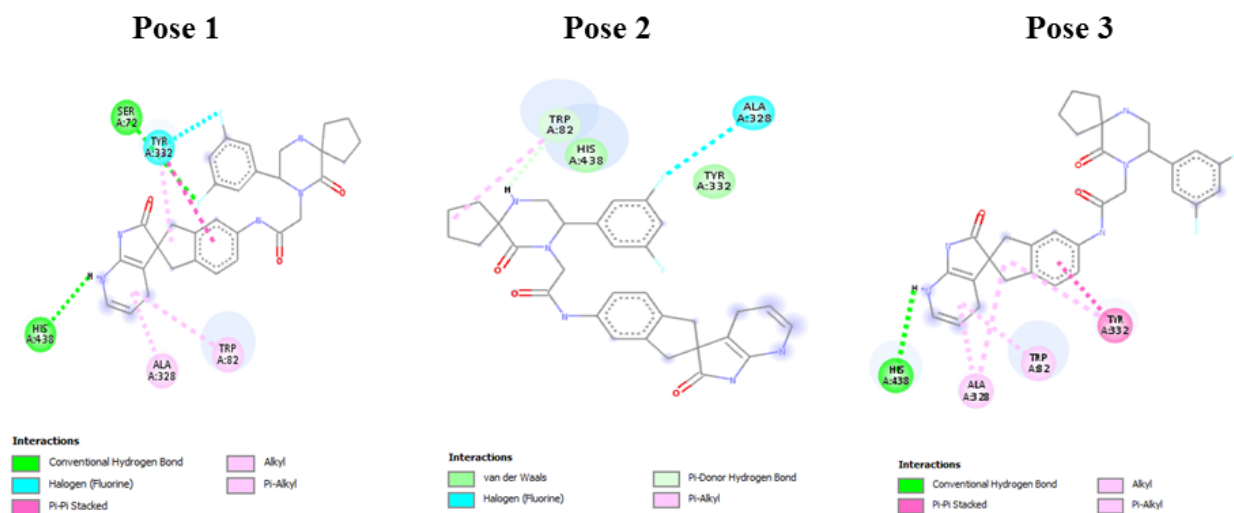


Figure S2. (d) The 2D interactions of the three best possible allosteric binding modes (poses) of the MK-3207 ligand with BuChE (1POI).

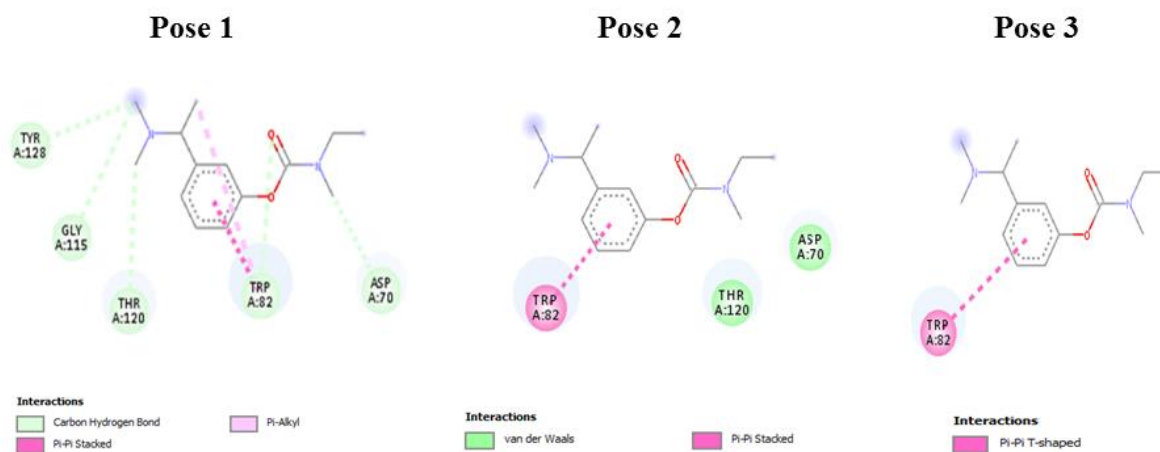


Figure S2. (e) The 2D interactions of the three best possible allosteric binding modes (poses) of the Rivastigmine (77991) ligand with BuChE (1POI).

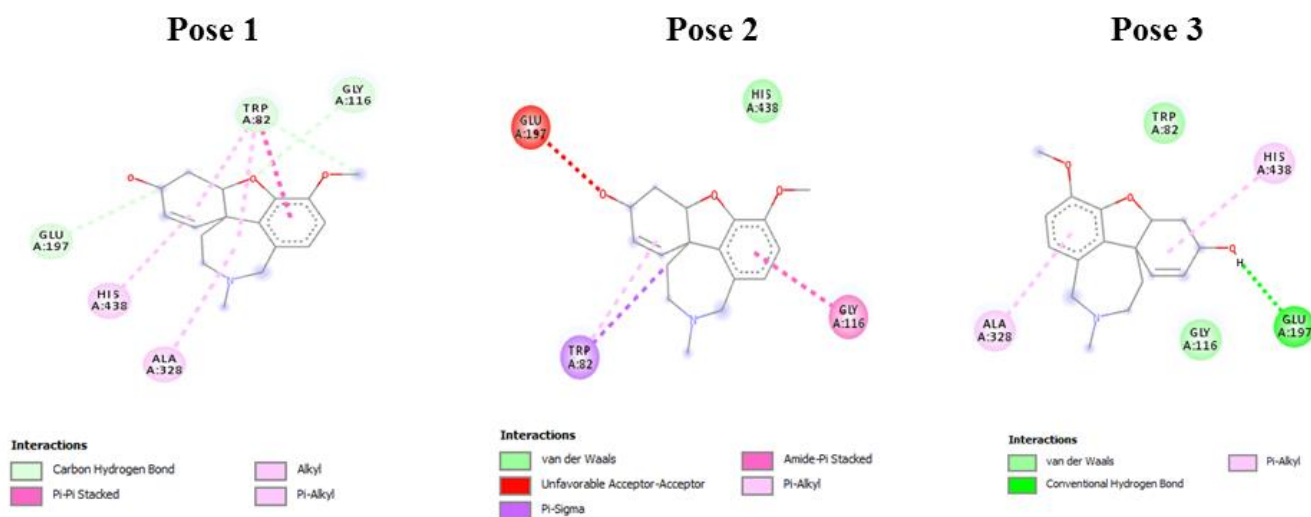


Figure S2. (f) The 2D interactions of the three best possible allosteric binding modes (poses) of the Galantamine (9651) ligand with BuChE (1P0I).

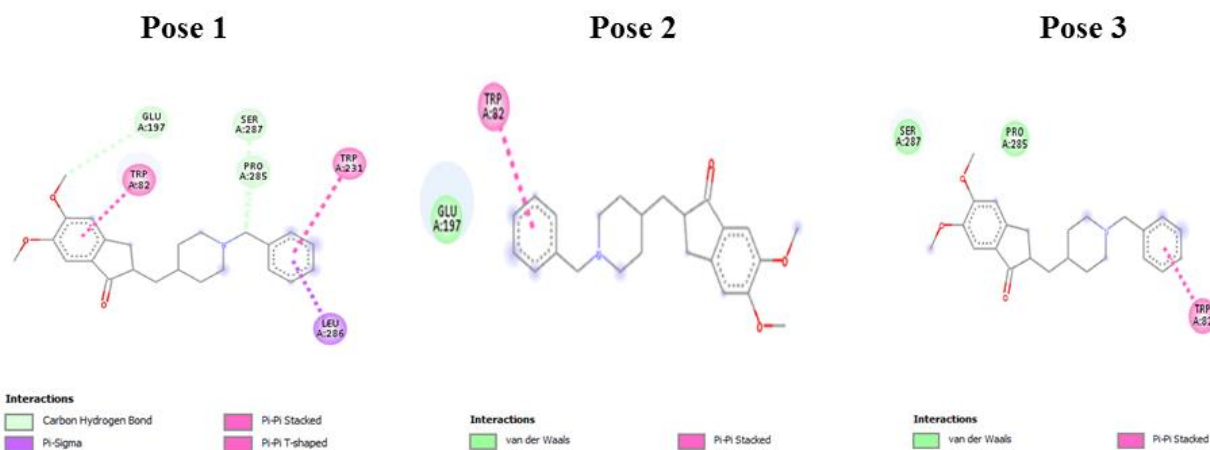


Figure S2. (g) The 2D interactions of the three best possible allosteric binding modes (poses) of the Donepezil (3152) ligand with BuChE (1P0I).

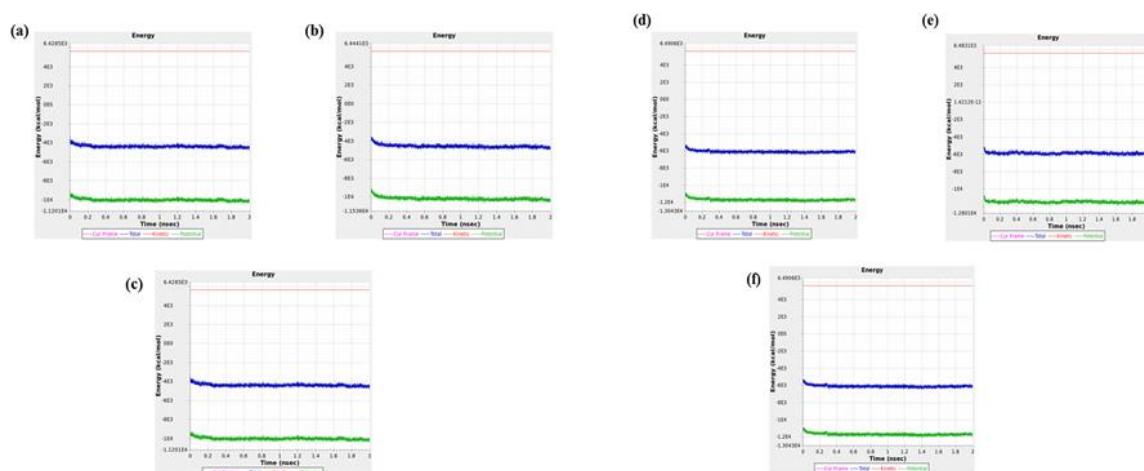


Figure S3. (A) The energy plot compounds of 7E3D with (a) Atogepant (b) Ubrogepant (c) MK-3207 (d) Rivastigmine (77991) (e) Galantamine (9651) (f) Donepezil (3152) during the simulation.

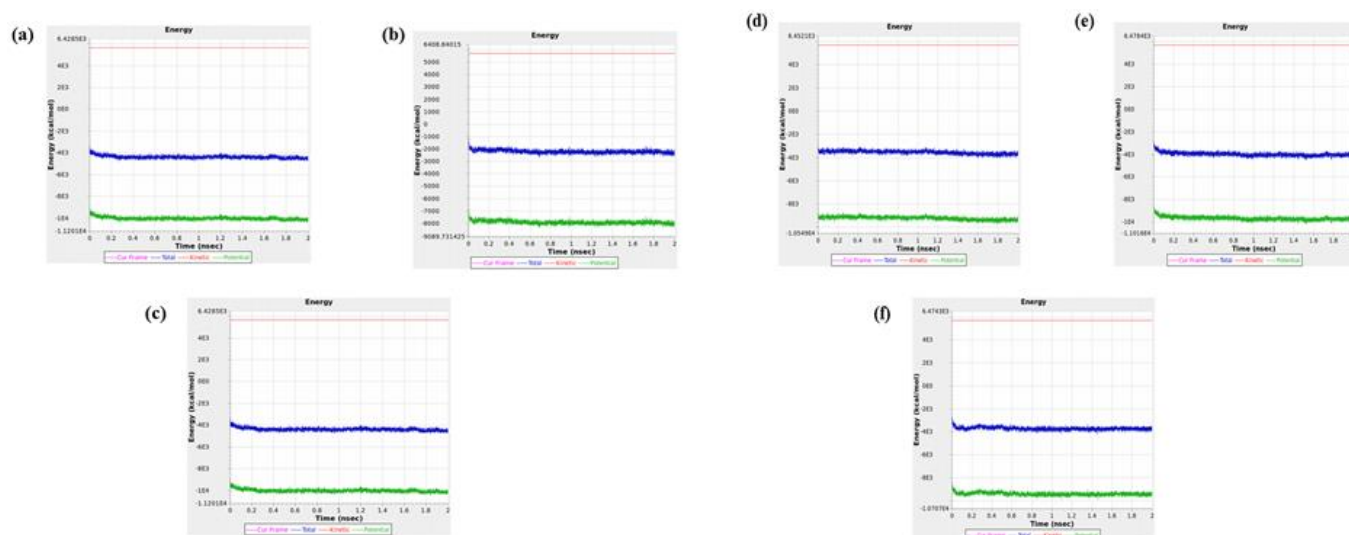


Figure S3. (B) The energy plot compounds of 1P0I with (a) Atogepant (b) Rimegepant (c) Ubrogapant (d) Rivastigmine (77991) (e) Galantamine (9651) (f) Donepezil (3152) during the simulation.